AMERICAN SOCIETY FOR MICROBIOLOGY | Journal of Virology®

VIRUS-CELL INTERACTIONS

Genome-Wide Screening Uncovers the Significance of N-Sulfation of Heparan Sulfate as a Host Cell Factor for Chikungunya Virus Infection

Atsushi Tanaka,[a,b] Uranan Tumkosit,[b] Shota Nakamura,[a] Daisuke Motooka,[a] Natsuko Kishishita,[a,b*] Thongkoon Priengprom,[b] Areerat Sa-ngasang,[c*] Taroh Kinoshita,[a,d] Naokazu Takeda,[a,b] Yusuke Maeda[a]

Research Institute for Microbial Diseases, Osaka University, Suita, Osaka, Japan[a]; Thailand-Japan Research Collaboration Center on Emerging and Re-emerging Infections, Department of Medical Sciences, Ministry of Public Health, Nonthaburi, Thailand[b]; Arbovirus Section, National Institute of Health, Department of Medical Sciences, Ministry of Public Health, Nonthaburi, Thailand[c]; WPI Immunology Frontier Research Center, Osaka University, Suita, Osaka, Japan[d]

ABSTRACT The molecular mechanisms underlying chikungunya virus (CHIKV) infection are poorly characterized. In this study, we analyzed the host factors involved in CHIKV infection using genome-wide screening. Human haploid HAP1 cells, into which an exon-trapping vector was introduced, were challenged with a vesicular stomatitis virus pseudotype bearing the CHIKV E3 to E1 envelope proteins. Analysis of genes enriched in the cells resistant to the pseudotyped virus infection unveiled a critical role of N-sulfation of heparan sulfate (HS) for the infectivity of the clinically isolated CHIKV Thai#16856 strain to HAP1 cells. Knockout of NDST1 that catalyzes N-sulfation of HS greatly decreased the binding and infectivity of CHIKV Thai#16856 strain but not infectivity of Japanese encephalitis virus (JEV) and yellow fever virus (YFV). While glycosaminoglycans were commonly required for the efficient infectivity of CHIKV, JEV, and YFV, as shown by using *B3GAT3* knockout cells, the tropism for N-sulfate was specific to CHIKV. Expression of chondroitin sulfate (CS) in *NDST1*-knockout HAP1 cells did not restore the binding of CHIKV Thai#16856 strain and the infectivity of its pseudotype but restored the infectivity of authentic CHIKV Thai#16856, suggesting that CS functions at later steps after CHIKV binding. Among the genes enriched in this screening, we found that TM9SF2 is critical for N-sulfation of HS and therefore for CHIKV infection because it is involved in the proper localization and stability of NDST1. Determination of the significance of and the relevant proteins to N-sulfation of HS may contribute to understanding mechanisms of CHIKV propagation, cell tropism, and pathogenesis.

IMPORTANCE Recent outbreaks of chikungunya fever have increased its clinical importance. Chikungunya virus (CHIKV) utilizes host glycosaminoglycans to bind efficiently to its target cells. However, the substructure in glycosaminoglycans required for CHIKV infection have not been characterized. Here, we unveil that N-sulfate in heparan sulfate is essential for the efficient infection of a clinical CHIKV strain to HAP1 cells and that chondroitin sulfate does not help the CHIKV binding but does play roles at the later steps in HAP1 cells. We show, by comparing previous reports using Chinese hamster ovary cells, along with another observation that enhanced infectivity of CHIKV bearing Arg82 in envelope E2 does not depend on glycosaminoglycans in HAP1 cells, that the infection manner of CHIKV varies among host cells. We also show that TM9SF2 is required for CHIKV infection to HAP1 cells because it is involved in the N-sulfation of heparan sulfate through ensuring NDST1 activity.

KEYWORDS TM9SF2, chikungunya, glycosaminoglycan, heparan sulfate

Received 15 March 2017 **Accepted** 3 April 2017

Accepted manuscript posted online 12 April 2017

Citation Tanaka A, Tumkosit U, Nakamura S, Motooka D, Kishishita N, Priengprom T, Sa-ngasang A, Kinoshita T, Takeda N, Maeda Y. 2017. Genome-wide screening uncovers the significance of N-sulfation of heparan sulfate as a host cell factor for chikungunya virus infection. J Virol 91:e00432-17. https://doi.org/10.1128/JVI.00432-17.

Editor Stanley Perlman, University of Iowa

Address correspondence to Yusuke Maeda, ymaeda@biken.osaka-u.ac.jp.

* Present address: Natsuko Kishishita, Center for Drug Design Research, National Institutes of Biomedical Innovation, Health and Nutrition, Ibaraki, Osaka, Japan; Areerat Sa-ngasang, Department of Medical Science, Ministry of Public Health, Nonthaburi, Thailand.

Chikungunya fever, a mosquito-borne disease caused by chikungunya virus (CHIKV), mainly occurs in Africa and in South and Southeast Asia (1). Recent outbreaks have occurred in the Indian Ocean islands of Mayotte, Mauritius, Réunion, and the Seychelles (266,000 cases in 2005 and 2006 in Réunion Island), India (1.4 to 6.5 million cases estimated in 2006 and 2007) (2–5), Malaysia (14,000 referred patients in 2006 to 2009) (6), and Thailand (more than 46,000 estimated cases in 2008 and 2009) (5, 7–9). Chikungunya fever has also spread to Europe and the Americas (10–12). CHIKV is classically transmitted by the tropical mosquito *Aedes aegypti*, but outbreaks and endemic infections occurring throughout the world are transmitted by *Aedes albopictus*, which is found in temperate climatic areas. The extension of the distribution of CHIKV is associated with the A226V mutation in the viral E1 glycoprotein, which allows the virus to be transmitted by *A. albopictus* (13). Therefore, the clinical importance of chikungunya fever is increasing. However, no specific antiviral drug treatment or commercial CHIKV vaccine is available.

The onset of chikungunya fever is sudden, with high fever, frequently accompanied by severe joint pain, muscle pain, headache, nausea, fatigue, and rash, usually occurring 2 to 12 days after the mosquito bite. The joint pain of chikungunya fever usually lasts for several days or may be prolonged for weeks. In some cases, joint pain can persist for several months or even years after the initial infection (1, 3, 11). Treatment focuses on the relief of these symptoms with anti-inflammatory drugs.

CHIKV is a member of the genus *Alphavirus* in the family *Togaviridae*. Alphaviruses are enveloped spherical particles with a diameter of 65 to 70 nm (14, 15). CHIKV has a single positive-stranded RNA genome of 11.8 kbp encoding four nonstructural and five structural proteins. The structural proteins are translated from a subgenomic 26S mRNA as a single polyprotein, which is processed into five structural proteins: capsid, E3, E2, 6K, and E1 (16). The mature CHIKV particle has 240 copies each of the E1 and E2 proteins, and these proteins assemble into 80 spikes consisting of trimerized heterodimers of E2 and E1 on the viral envelope membrane (17). It has been reported that alphaviruses infect their target cells via receptor-mediated endocytosis and subsequent membrane fusion in acidic endosomes (18). The E1 and E2 glycoproteins are mainly responsible for viral fusion to the endosomal membrane and receptor binding, respectively (15, 19–23).

To identify the host factors that affect the early phase of CHIKV infection, we took a genetic approach, using knockout cell libraries constructed by the transfection of HAP1 cells, a haploid human cell line, with a *piggyBac*-transposon-based exon-trapping vector. Combining such knockout cell libraries with deep sequencing has recently been used to clarify the factors required by a variety of pathogens, including viruses, bacteria, and bacterial toxins (24–28). The exon-trap-mutagenized HAP1 cells were challenged with pseudotyped vesicular stomatitis virus (VSV) expressing the CHIKV E2/E1 envelope proteins instead of the VSV G protein, and the surviving cells were analyzed. Candidate genes were selected based on the numbers of sites into which the exon-trapping vector had been inserted compared to the unchallenged control cell pool. To test whether these genes are truly involved in CHIKV infection, knockout cells for each gene were established with the CRISPR/cas9 system and analyzed. In this way, we determined the minimum heparan sulfate (HS) structure, N-sulfated HS that is essential for efficient CHIKV infection, and identified several genes involved in N-sulfated HS biosynthesis and/or expression, other than those encoding enzymes known to catalyze HS biosynthesis.

RESULTS

Genome-wide screening of host factors critical for CHIKV infection. To identify the host factors required for CHIKV infection, we constructed an insertional mutant HAP1 library with a complexity of about 10^8 independent clones, using a *piggyBac*-transposon-based exon-trapping vector (29). The mutant library cells were challenged with VSVΔG*-CHIKV-E (multiplicity of infection [MOI] = 3) three times at 3-day intervals, which concentrated the infection-resistant target cell population. In the target and control cell populations, the genomic DNA adjacent to the inserted exon-trapping vector was

TABLE 1 Genes involved in CHIKV infection that are identified with genome-wide screening[a]

FDR	Enriched candidate gene	#	§	‡	FDR for genes reported by Jae et. al. (‡)
1.87E-235	EXT1				0
1.94E-129	TM9SF2				2.67E-138
1.70E-127	EXT2				3.14E-164
1.46E-68	COG5				5.81E-47
2.29E-66	PTAR1				4.90E-263
9.32E-64	TMEM165				2.18E-62
1.99E-61	COG3				4.43E-21
2.26E-37	TMED10				0.898
1.82E-26	COG4				1.42E-50
3.60E-26	COG6				3.72E-14
4.01E-24	NDST1				1.57E-233
1.08E-22	SLC10A7				0.893
1.05E-20	SLC39A9				0.00199
8.25E-19	COG7				9.60E-68
5.17E-17	COG2				1.96E-13
6.59E-15	MIA3				1
7.97E-12	TMED2				0.24
1.12E-11	MON2				1
9.75E-11	EXTL3				1.24E-311
2.70E-08	SACM1L				3.05E-15
0.000177	FAM20B				5.04E-29
0.000181	COG1				7.69E-10
0.000288	KIAA1432				1
0.000752	MBTPS2				1
0.00128	COG8				
0.00267	TM9SF3				1
0.00898	ARHGEF26				
0.032	ROCK2				1
0.0479	B3GAT3				6.78E-103

[a]Shaded columns: #, enzymes in the HS biosynthetic pathway; §, genes associated with congenital disorders of glycosylation; ‡, HS expression-related genes reported by Jae et al. (27).

amplified using splinkerette-PCR (91) and subjected to a deep-sequencing analysis with next-generation sequencing. The number of different sites at which the exon-trapping vector was inserted was counted in each gene. By comparing the numbers similarly counted in the control cells, which were not challenged with VSVΔG*-CHIKV-E, 29 genes with significantly increased numbers of insertion sites were identified in the target cell population (false discover rate [FDR] $<$ 0.05) as enriched candidate genes (Table 1). They encoded proteins that were classified into three categories: enzymes known to catalyze HS biosynthesis (six genes), nonenzymatic proteins reported previously (27) as related to HS expression (12 genes), and genes whose relationship with the HS pathway is unknown (11 genes). Exostosin 1 and 2 (EXT1 and EXT2), bifunctional heparan sulfate *N*-deacetylase/*N*-sulfotransferase 1 (NDST1), exostosin-like 3 (EXTL3), glycosaminoglycan xylosylkinase (FAM20B), and β-1,3-glucuronyltransferase 3 (B3GAT3) are enzymes involved in HS biosynthesis (Fig. 1). The components of the conserved oligomeric Golgi complex (COG1 to COG8), transmembrane protein 165 (TMEM165), transmembrane 9 superfamily member 2 (TM9SF2), protein prenyltransferase alpha subunit repeat-containing protein 1 (PTAR1), zinc transporter ZIP9 (SLC39A9), and phosphatidylinositide phosphatase SAC1 (SACM1L) are nonenzymatic proteins related to HS expression (27) (Table 1). The *COG* family and *TMEM165* genes are associated with congenital disorders of

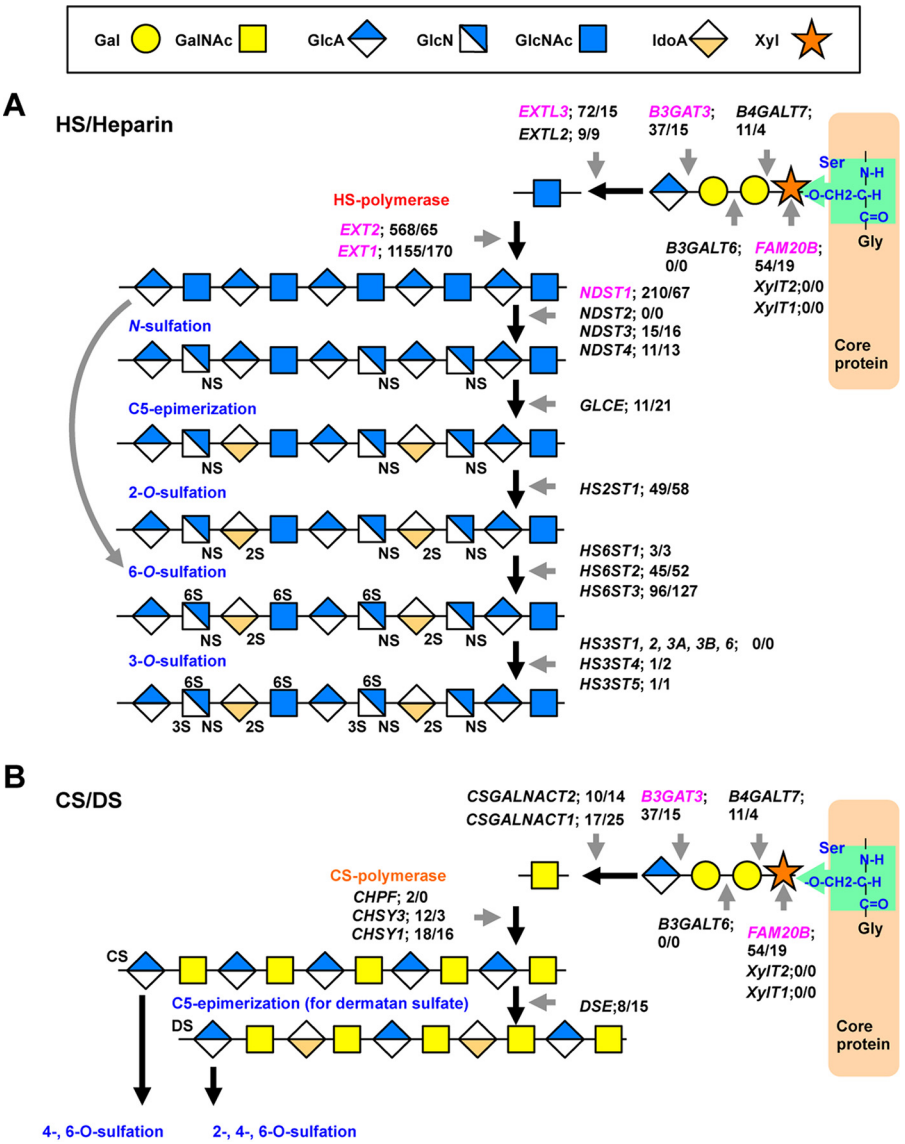

FIG 1 Overview of the heparan sulfate (HS)/heparin (A) and chondroitin sulfate (CS)/dermatan sulfate (DS) (B) biosynthetic pathways. The numbers shown in each gene represent the numbers of different integration sites at which the exon-trapping vector was inserted in each gene and are expressed as the numbers in the target cell population/the numbers in the control cell population. Genes that were significantly enriched in the target cell population (FDR $<$ 0.05 [shown in Table 1]) are indicated in red.

glycosylation (30–33). Our results clearly indicate the significance of HS in CHIKV infection. The third category included several genes encoding proteins involved in protein trafficking, such as *MIA3*, *TMED2*, *TMED10*, and *MON2*, and genes associated with GTPase molecules, such as *KIAA1432*, *ARHGEF26*, and *ROCK2*. The relationships of these genes in the third category to CHIKV infection were analyzed with VSV-pseudotyped CHIKV-E and authentic CHIKV Thai#16856 strain. These knockout cells showed some degree of resistance to the pseudotyped virus infection but were sensitive to authentic CHIKV Thai#16856 strain similarly to wild-type HAP1 cells, suggesting that proteins in the third category are involved in the life cycle of VSV but not CHIKV entry (data not shown).

N-sulfated HS is the minimum structure essential for efficient CHIKV infection. Most genes encoding the enzymes that catalyze the steps in HS biosynthesis from the beginning of the modification to the N-sulfation of glucosamine were identified as critical host factors when the genes were interrupted by the exon-trapping vector

(*FAM20B*, *B3GAT3*, *EXTL3*, *EXT1*, *EXT2*, and *NDST1*, but not *B4GALT7*, which still showed $P = 0.02$ in a Fisher exact test) (Fig. 1). However, no genes encoding enzymes that act after the N-sulfation step, which is catalyzed by NDST1, were identified as enriched (Fig. 1). D-Glucuronyl C5-epimerase (GLCE) is the only enzyme that acts downstream of NDST1 and catalyzes the C5 epimerization of D-glucuronic acid (GlcA) to L-iduronic acid (IdoA). Notably, *GLCE* was not enriched, even though a significant number of exon-trapping vectors were inserted into it in the control cells, indicating that GLCE is not a critical molecule for CHIKV infection. To verify that NDST1 is essential and that GLCE is nonessential for efficient CHIKV infection, we established *B3GAT3*-, *NDST1*-, and *GLCE*-knockout HAP1 cells (HAP1ΔB3GAT3, HAP1ΔNDST1, and HAP1ΔGLCE, respectively) using the CRISPR/Cas9 system and their rescued cells (Fig. 2A). Clone F58-10E4 mouse monoclonal antibody (MAb) was used to evaluate the amount of N-sulfated HS expressed on the cell surfaces, because N-sulfated glucosamine is an epitope of F58-10E4. In the HAP1ΔB3GAT3 and HAP1ΔNDST1 cells, surface N-sulfated HS expression was completely lost, as expected, whereas HAP1ΔGLCE cells expressed a significant amount of N-sulfated HS, although the level was somewhat lower than that in the wild-type cells (Fig. 2A). The reason why HS expression was reduced in the absence of GLCE was not clear, but full activity of NDST1 may require GLCE by a complex formation or mature HS products beyond the modification by GLCE for a feedback regulation. The impaired expression of N-sulfated HS was restored in the rescued cells, into which the individual knocked-out genes were stably reintroduced (Fig. 2A). These cells were challenged with VSVΔG-luci-CHIKV-E (Thai#16856 and Ross strains). CHIKV Thai#16856 and ROSS strains were used as the templates to construct VSVΔG*-CHIKV-E bearing CHIKV envelope proteins E1 to E3. Authentic CHIKV Thai#16856 used in this study was verified by sequencing to have only one different amino acid (glutamine 252) from that of CHIKV-LR strain (lysine 252), a common clinical isolate (GenBank accession no. EU224268.1), in the E2/E1 sequence. This variation (K to Q) causes a loss of positive charge which is usually favorable for GAG binding and was observed in 32 CHIKV strains among 159 strains recorded in the UniProt database, most of which are clinical isolates. Thus, the Thai#16856 strain we used in this study was considered to be a clinical isolate. CHIKV Ross strain, which is a prototype CHIKV strain from the Central/East African clade (34), was also used in this study to construct pseudoviruses but not as an authentic virus, and the E2/E1 sequence was verified not to have any mutation in the original sequence recorded (GenBank accession no. AF490259). As shown in Fig. 2B, HAP1ΔB3GAT3 and HAP1ΔNDST1 cells showed significantly reduced susceptibility to the VSVΔG-luci-CHIKV-E (Ross and Thai#16856 strains) >10-fold that of the parental wild-type HAP1 cells, but HAP1ΔGLCE showed much weaker reduction of the susceptibility which seemed to be brought by the mildly reduced expression of N-sulfated HS (Fig. 2A). Survival of cells challenged with VSVΔG*-CHIKV-E (Ross and Thai#16856 strains) was observed in HAP1ΔNDST1 cells but not in HAP1ΔGLCE cells (Fig. 2C). Next, the susceptibilities of these HAP1-derived mutant cells to the clinically isolated authentic CHIKV Thai#16856 strain and other mosquito-borne arboviruses were examined (Fig. 2D). Sindbis virus (SINV) Ar-339 strain, Japanese encephalitis virus (JEV) JaGAr strain, and yellow fever virus (YFV) vaccine strain 17D were known to utilize cell surface glycosaminoglycans for their binding to the target cells, as well as CHIKV (35–37). Like VSVΔG*-CHIKV-E, the CHIKV Thai#16856 strain showed a significantly reduced infectivity to HAP1ΔB3GAT3 and HAP1ΔNDST1 cells, being about 100- and 400-fold lower, respectively, than that of wild-type HAP1 cell, whereas HAP1ΔGLCE cells showed no significant difference in the susceptibility from wild-type HAP1 cells. On the other hands, JEV and YFV, which both belong to genus *Flavivirus*, showed greatly reduced infectivity only to HAP1ΔB3GAT3 cells and not to HAP1ΔNDST1 and HAP1ΔGLCE cells compared to wild-type HAP1 cells. SINV showed significant reduction of infectivity to HAP1ΔB3GAT3 and HAP1ΔNDST1 cells, and yet the infectivity to HAP1ΔNDST1 cells was stronger than that of CHIKV Thai#16856 (Fig. 2D and see also Fig. 5I). Thus, GAG biosynthesis are critical for all four virus strains, but a significant reduction of susceptibility to HAP1ΔNDST1 cells was most prominent in CHIKV infection. These

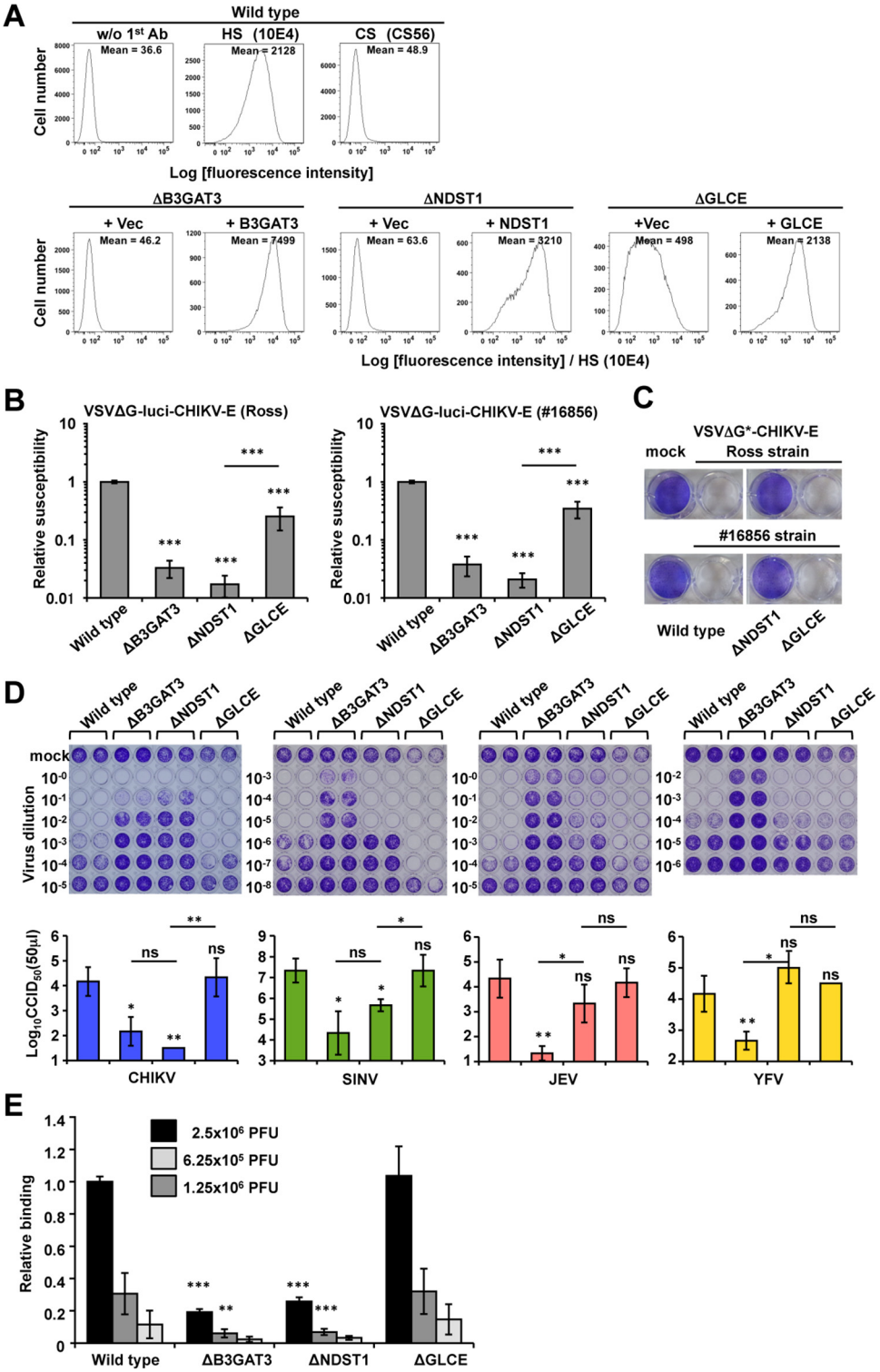

FIG 2 Susceptibilities of GAG-deficient HAP1-knockout cells to CHIKV and mosquito-borne viruses. (A) The cell surface expressions of HS and CS were analyzed by flow cytometry using anti-HS MAb (F58-10E4) or anti-CS MAb (CS56) in wild-type HAP1 cells and *B3GAT3*-, *NDST1*-, and *GLCE*-knockout HAP1 cell lines stably transfected with either vector expressing the corresponding gene (+*B3GAT3*, +*NDST1*, or +*GLCE*) or empty vector (+Vec). The geometric mean fluorescence intensity (G-MFI) for each cell line is shown. (B) Wild-type HAP1, HAP1ΔB3GAT3, HAP1ΔNDST1, and HAP1ΔGLCE cells that had been plated 1 day earlier were inoculated with VSVΔG-luci-CHIKV-E (Ross or Thai#16856 strain), and the luciferase activity was measured 1 day after the inoculation. RThe relative susceptibility was calculated as the ratio of the luciferase activity in the knockout cells to that in the wild-type HAP1 cells. Bars indicate means ± the standard deviations (SD) for three independent experiments. (C) Infection of wild-type HAP1, HAP1ΔNDST1, and HAP1ΔGLCE cells with VSVΔG*-CHIKV-E (Ross or Thai#16856 strain; MOI > 10).

(Continued on next page)

results demonstrated that the N-sulfate in HS is critical for efficient CHIKV infection of HAP1 cells and that this tropism for N-sulfate is specific to CHIKV among the four arboviruses examined here, suggesting that the binding of CHIKV to GAGs depends on specific structural affinities rather than on simple electrostatic forces. C5 epimerization of HS by GLCE, which is not essential for CHIKV infection, as described above, is required for the subsequent 2-O-sulfation and most likely 3-O-sulfation of HS, suggesting their nonessentiality for CHIKV infection (see Discussion). 6-O-Sulfation, which occurs independently of N-sulfation with less efficiency, did not rescue the inefficient CHIKV infection of the HAP1ΔNDST1 cells as well. Therefore, O-sulfates are not necessary or insufficient for efficient CHIKV infection, although we cannot exclude the possibility that O-sulfates enhances CHIKV infection in the presence of N-sulfates. SINV, JEV, and YFV may use CS or remaining 6-O-sulfate of HS more efficiently for their infection to HAP1ΔNDST1 cells than CHIKV does. Because the idea that GAGs function as the surface receptors for viral infection is widely accepted, we examined whether the N-sulfation of HS is critical for CHIKV to bind to the cell surface. The binding of purified CHIKV virion to HAP1ΔB3GAT3 and HAP1ΔNDST1 cells decreased 12 and 20%, respectively, compared to that in intact HAP1 cells, whereas CHIKV binding to HAP1/ΔGLCE cells was normal, which is consistent with the susceptibility of these cells to CHIKV (Fig. 2E). Therefore, N-sulfated HS is the minimum structure essential for efficient CHIKV binding and infection.

CS enhances CHIKV infectivity after the binding and entry to the HAP1 cells. Because CS is also reported to function as a receptor for CHIKV and because HAP1 cells express relatively low amount of CS (Fig. 2A), which could explain why we did not detect genes involved in CS biosynthesis with genome-wide screening, we reevaluated the significance of CS in CHIKV infection. The overexpression of CSGALNACT1, which catalyzes the addition of the first *N*-acetyl galactosamine to GlcA in the GAG stem, and CS elongation caused significant surface expression of CS in HAP1ΔNDST1 cells lacking N-sulfated HS, which was evaluated by the staining with CS56 MAb that recognizes the GAG portion of CS (CS-A and CS-C). Therefore, these cells were suitable for analyzing the role of CS in CHIKV infection (Fig. 3A). The surface CS expression on HAP1ΔNDST1 cells induced by the overexpression of CSGALNACT1 (HAP1ΔNDST1+CSGALNACT1) did not rescue the decreased susceptibility of HAP1ΔNDST1 cells to VSVΔG-luci-CHIKV-E (Thai#16856) pseudovirus (Fig. 3B). In addition, surface binding of authentic CHIKV (Thai#16856) to the HAP1ΔNDST1 cells was significantly increased by reexpression of NDST1 but not CSGALNACT1 (Fig. 3C). These results indicated that the surface expression of CS did not function as a binding receptor for CHIKV. Finally, infectivity of authentic CHIKV (Thai#16856) to the HAP1 cells expressing or not expressing CS in the absence of N-sulfated HS was examined. Surprisingly, in contrast to the results presented above that the infectivity of pseudovirus and binding of authentic virion did not depend on CS expression, the infectivity of authentic CHIKV Thai#16856 was enhanced in the presence of CS expression (HAP1ΔNDST1+CSGALNACT1 cells) to an extent similar to that observed in the presence of N-sulfated HS (HAP1ΔNDST1+NDST cell), suggesting that CS play roles at the later steps after the CHIKV binding and entry to the HAP1 cells (Fig. 3D).

FIG 2 Legend (Continued)
The cells were fixed and stained with crystal violet 4 days after inoculation. (D) Wild-type HAP1, HAP1ΔB3GAT3, HAP1ΔNDST1, and HAP1ΔGLCE cells were infected with serially diluted CHIKV Thai#16856 strain, SINV, JEV, or YFV. Cell viability was measured by using WST-1 reagent, and the susceptibility of each cell to these viruses is shown by the virus titers ($CCID_{50}$/50 μl, determined using a Reed-Muench calculation) 4 days after inoculation as described in Materials and Methods. The cells were fixed and stained with crystal violet. (E) CHIKV binding to GAG-related gene knockout cells. Nearly confluent wild-type HAP1, HAP1ΔB3GAT3, HAP1ΔNDST1, and HAP1ΔGLCE cells seeded in a 96-multiwell plate were incubated with purified CHIKV Thai#16856 strain (2.5×10^6, 1.25×10^6, or 6.25×10^5 PFU) at 4°C for 1 h. The cells were then washed, fixed, and stained with a CHIKV-specific mouse antibody and horseradish peroxidase-conjugated goat anti-mouse immunoglobulin antibody. Relative binding was calculated as the ratio to the wild-type HAP1 cells with 2.5×10^6 PFU CHIKV. The data represent the means ± the SD for three independent experiments. Statistical significances for $CCID_{50}$/50 μl between wild-type HAP1 and HAP1 mutants or between various mutant cell lines (shown on the horizontal bars) were evaluated by using an unpaired, two-tailed *t* test (*, $P < 0.05$; **, $P < 0.01$; ***, $P < 0.001$; ns, not significant).

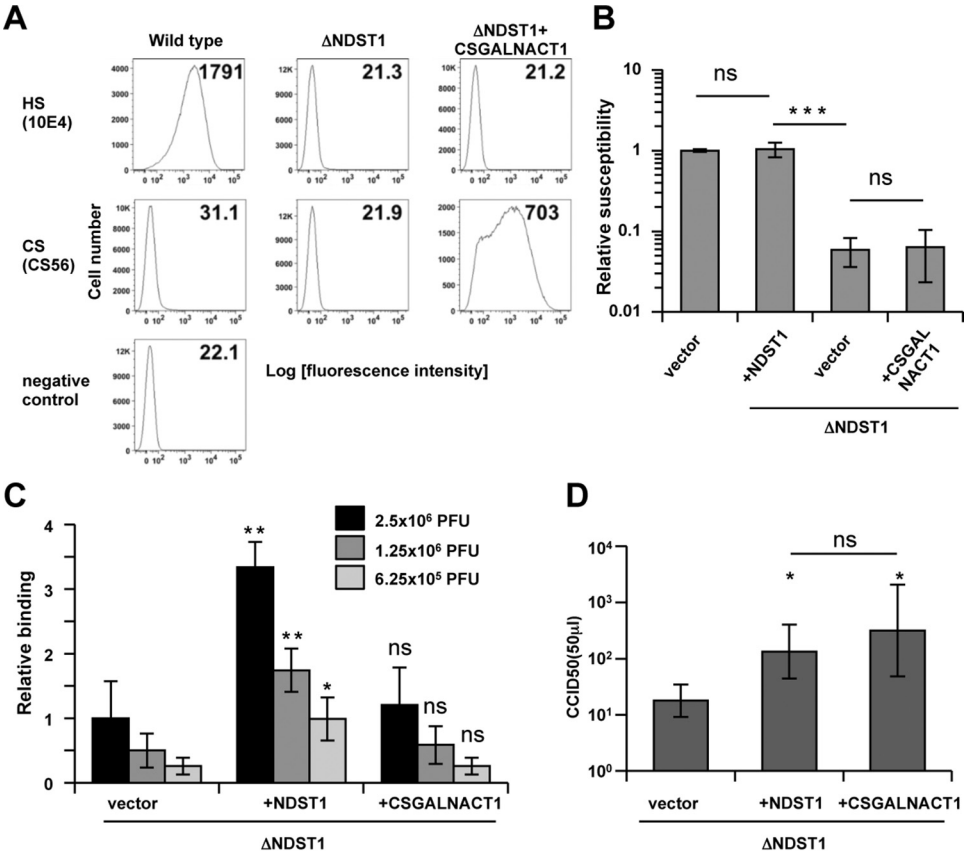

FIG 3 Contribution of cell surface CS to CHIKV infection. (A) Establishment of HAP1 cells stably expressing CS but not N-sulfated HS. HAP1ΔNDST1 cells were infected with a retrovirus bearing the CSGALNACT1 gene. Cell surface expressions of CS and HS were examined with flow cytometry using CS56 and F58-10E4 antibodies, respectively. Cells stained with only secondary antibody (Alexa 488-conjugated anti-mouse IgM antibody) were used as a negative control. The G-MFIs are shown. (B) HAP1+vector (empty vector), HAP1ΔNDST1+vector, HAP1ΔNDST1+NDST1, and HAP1ΔNDST1+CSGALNACT1 cells were inoculated with VSVΔG-luci-CHIKV-E (Thai#16856 strain). The luciferase activity was measured 1 day after incubation. The relative susceptibilities were calculated as ratios of the luciferase activities in these cells to those in wild-type HAP1+vector cells. The data represent the means ± the SD for four independent experiments. Statistical significances between pairs of data were analyzed by using an unpaired, two-tailed *t* test (***, $P < 0.001$; ns, not significant). (C) CHIKV binding to HAP1ΔNDST1+vector, HAP1ΔNDST1+NDST1, and HAP1ΔNDST1+CSGALNACT1 cells. The experiment was done in the same way as Fig. 2E. Relative binding was calculated as the ratio to the HAP1ΔNDST1+vector cells with 2.5×10^6 PFU CHIKV. The data represent the means ± the SD for three independent experiments. Statistical significances against HAP1ΔNDST1+vector cells were evaluated by using an unpaired, two-tailed *t* test (*, $P < 0.05$; **, $P < 0.01$; ***, $P < 0.001$; ns, not significant). (D) HAP1ΔNDST1 derivative cells were infected with serially diluted CHIKV Thai#16856 strain, and the experiment was performed as described for Fig. 2D. The data represent the means ± the SD for four independent experiments. Statistical significances for $CCID_{50}$/50 μl between HAP1ΔNDST1+vector and other mutants or between various rescued cell lines (shown on the horizontal bar) were evaluated by using an unpaired, two-tailed *t* test (*, $P < 0.05$; ns, not significant).

Genes other than enzymes that catalyze HS biosynthesis are involved in multiple glycosylation pathways, including HS glycosylation. The *COG* family members, *TMEM165*, *TM9SF2*, *PTAR1*, *SLC39A9*, and *SACM1L* that were identified in this study have also been selected in a previous report as statistically significant candidates when genome-wide screening using HAP1 cells focused on the expression of N-sulfated HS evaluated by the staining with the F58-10E4 antibody, which we used in this study; however, the authors did not confirm that the defects in these genes truly affected the expression of N-sulfated HS and did not characterize them more in detail (27). The COG complex regulates vesicular trafficking, predominantly intra-Golgi retrograde transport (38), and TMEM165 is a calcium (and probably manganese)/proton exchanger involved in lysosomal and Golgi ion homeostasis (39). PTAR1 belongs to the protein prenyltransferase subunit alpha family. TM9SF2 and SLC39A9 may be transporters based on their structures, although their actual functions are still unclear. We examined whether the

surface expression of N-sulfated HS was indeed affected by defects in these genes. To this end, knockout cells of each gene, established with the CRISPR/Cas9 system, and their rescued cells, which were established by transfecting each cell line with the corresponding gene, were analyzed with flow cytometry. As expected, all the knockout cells showed reduced surface expression of N-sulfated HS, but to various extents (Fig. 4A and B). The susceptibility of these knockout cells to CHIKV infection was analyzed using both VSVΔG-luci-CHIKV-E pseudovirus and authentic CHIKV. *B3GAT3* and *NDST1* knockout reduced infection by the CHIKV pseudotype by more than 90%; the knockout of *COG7*, *TMEM165*, and *TM9SF2* reduced it by about 80%; and the knockout of *SLC39A9* reduced it by about 60% (Fig. 4C). When authentic CHIKV was used to infect the cells, the *B3GAT3*-, *NDST1*-, and *TM9SF2*-knockout cells were most resistant to infection (Fig. 4D). These results are roughly consistent with the reduced levels of HS expression in these cells. Because it was not known whether PTAR1, TM9SF2, and SLC39A9 are involved in only the HS glycosylation pathway, we examined whether other glycosylation pathways were affected by their defects, which could partly explain the reduced susceptibility of the knockout cells to CHIKV. To this end, various glycosylation pathways were analyzed by treating the knockout cells with cholera toxin B (40) and several lectins, including *Helix pomatia* agglutinin (41), soybean agglutinin (SBA) (42), peanut agglutinin (PNA) (43), and *Griffonia simplicifolia* lectin II (GSII) (44) (Fig. 4E). Cholera toxin B subunit specifically binds GM1, a glycosphingolipid with monosialylation. PNA binds asialo-galactose-β-1,3-*N*-acetylgalactosamine (asialo-GalNAc), which is often detected in the impaired O-glycosylation and glycosphingolipid pathways. SBA binds terminal GalNAc and, to a lesser extent, the galactose residue present in the immature O-glycans and glycosphingolipids. GSII binds highly selectively to the terminal nonreducing GlcNAc residues of glycoproteins. As expected, the knockout of *COG7*, *PTAR1*, or *SLC39A9* strongly affected multiple glycosylation pathways. The knockout of *TM9SF2* or *TMEM165* caused rather mild abnormalities, but also in multiple pathways. Therefore, proteins other than the enzymes catalyzing HS biosynthesis are involved in multiple glycosylation pathways, including that of HS.

TM9SF2 is a Golgi apparatus-resident protein critical for the correct localization and stability of NDST1. TM9SF2 is a well-conserved protein in mammals, but its function is unknown. Because the knockout of *TM9SF2* strongly affected the expression of N-sulfated HS in a relatively specific manner and reduced the susceptibility of cells to CHIKV infection as mentioned above, we investigated the mechanism by which TM9SF2 regulates the expression of N-sulfated HS. First, to check whether the expression of proteoglycans bearing GAGs was affected by the TM9SF2 defect, the surface expression of syndecan and glypican, major source of GAGs in HAP1 cells, was examined, but no significant reduction in their expression was observed (Fig. 5A). Indirect immunofluorescence microscopy showed that TM9SF2 was clearly colocalized with GM130 and Golgin97, Golgi marker proteins, which is consistent with the biosynthesis of HS in the Golgi compartment, although some was also expressed on the cell surface (Fig. 5B and C). We next examined the glycosylation of glypican-3, which possibly contains two HS and two N-glycan chains. Since the HS chain is huge and diverse, the glypican-3 band on an SDS-PAGE gel is normally smeared and not clear (Fig. 5D). However, in HAP1ΔB3GAT3 cells, which are deficient in the elongation of disaccharide repeats, the band was readily detected as an almost single band of ~70 kDa (Fig. 5D, white arrow). Interestingly, the HAP1ΔNDST1 and HAP1ΔTM9SF2 cells, but not their rescued cells, showed similar discrete but still broad bands of ~200 to ~250 kDa for glypican-3 (Fig. 5D, black arrow), whereas the other knockout cells showed no significant bands, suggesting that the defective HS synthesis in HAP1ΔTM9SF2 cells arises from the impaired function of NDST1. To examine this possibility, we performed a heparinase III digestion assay. Heparinase III is an endoglycosidase that cleaves the linkages between N-sulfated or N-acetylated glucosamine and glucuronic acid and thus trims HS chains, resulting in the production of ΔDi-GlcA at the end of the chain, which is specifically recognized by the 3G10 MAb. This antibody allowed us to measure the number of HS chains, and the 10E4 antibody allowed us to measure amount of

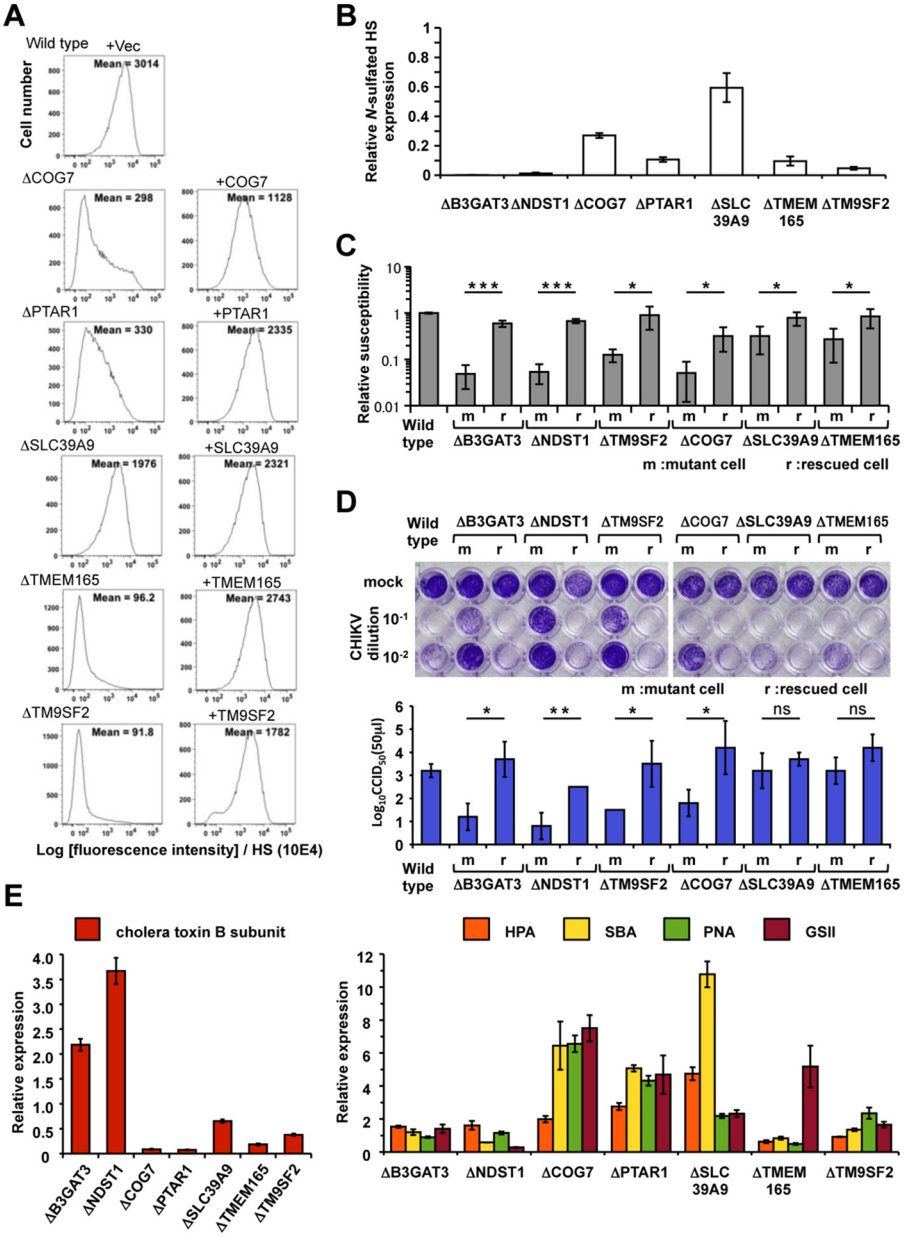

FIG 4 Contribution of HS expression-related genes to cell susceptibility to CHIKV. (A) Each knockout cell line was stably introduced with each appropriate gene responsible for the knockout (rescued cell) or empty vector (mutant cell) through retrovirus-based infection. The cell surface expression of HS in the rescued cells (+TM9SF2, +SLC39A, +TMEM165, or +COG7) or the mutant cells (+Vec) was analyzed by flow cytometry with anti-HS MAb (F58-10E4). (B) The effects of gene knockout on the cell surface expression of N-sulfated HS are shown as the ratios of the G-MFIs of mutant cells to those of rescued cells in individual knockout cell lines. The data represent the means ± the standard errors (SE) for four to five independent experiments. (C) Effects of gene knockout on the susceptibilities of cells to CHIKV pseudovirus. Rescued and mutant cells were inoculated with VSVΔG-luci-CHIKV-E (Thai#16856 strain), and the luciferase activities were measured (see Materials and Methods). (D) The susceptibilities of knockout cells to authentic CHIKV Thai#16856 strain were examined. Rescued and mutant cells for each gene were inoculated with CHIKV Thai#16856 strain, and the experiment was performed as described for Fig. 2D. The data represent the means ± the SD for three independent experiments. The statistical significances of $CCID_{50}$/50 μl between mutant and rescued cells were evaluated by using an unpaired, two-tailed *t* test (*, $P < 0.05$; **, $P < 0.01$; ***, $P < 0.001$; ns, not significant). (E) The surface expression of various types of glycosylation on individual HAP1 knockout cells was examined by flow cytometry using cholera toxin B subunit (left panel), and *Helix pomatia* agglutinin (HPA), soybean agglutinin (SBA), peanut agglutinin (PNA), and *Griffonia simplicifolia* lectin II (GSII) (right panel). The effects of gene knockout on cell surface glycosylation are shown as the ratios of the G-MFIs of the mutant cells to those of rescued cells in individual knockout cell lines. The data represent the means ± the SE of two to five independent experiments.

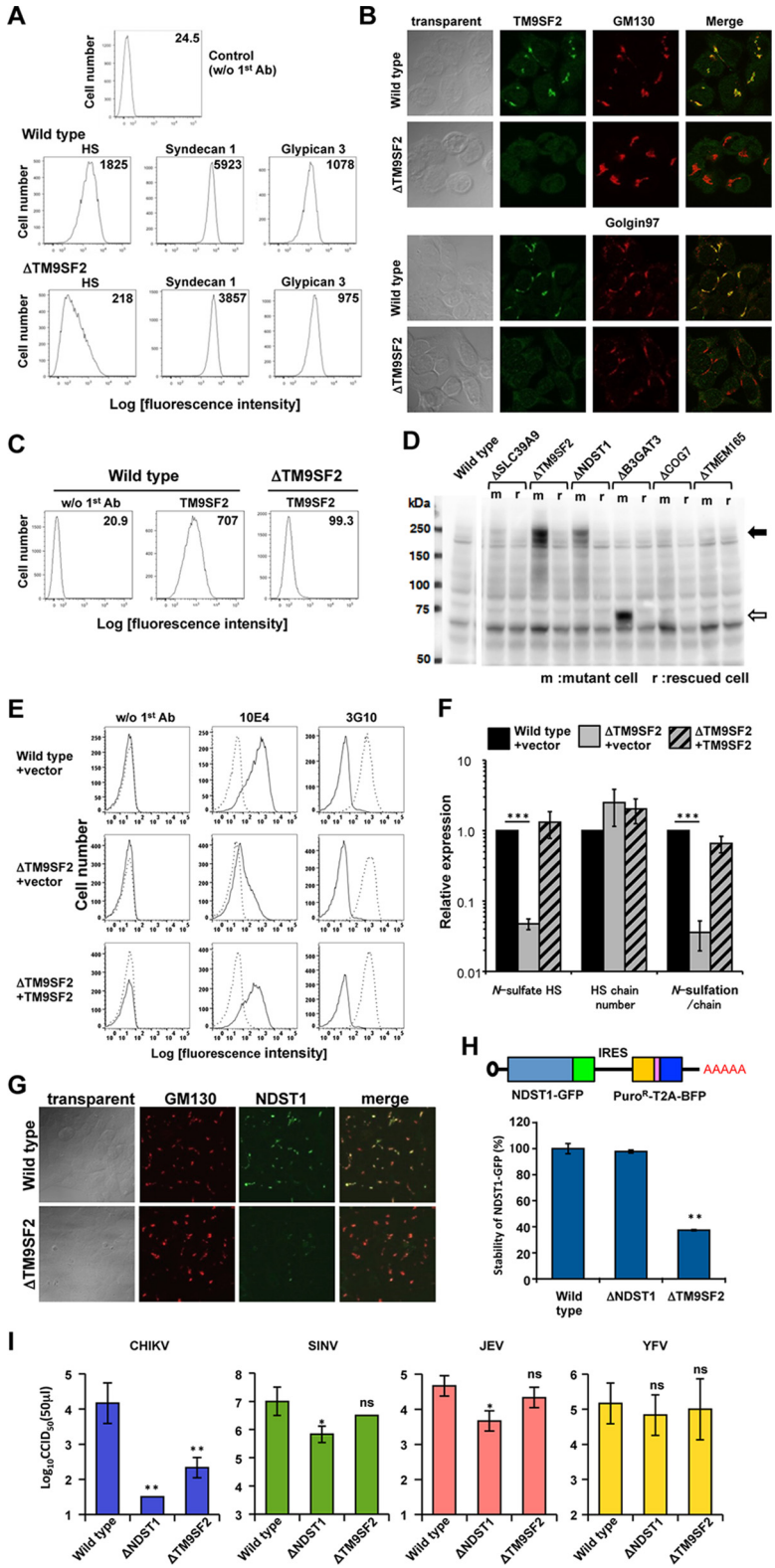

FIG 5 Golgi compartment-resident TM9SF2-dependent localization and stability of NDST1. (A) The cell surface expressions of HS, syndecan-1, and glypican-3 in wild-type HAP1 and HAP1ΔTM9SF2 cells were analyzed by flow cytometry. The numbers indicate the G-MFIs. (B) Intracellular localization of endogenous TM9SF2. Cells were methanol fixed and double stained with anti-TM9SF2, anti-GM130, or anti-Golgin97 antibodies. Green, TM9SF2; red, GM130 or Golgin97 (Golgi apparatus markers). (C) The cell surface expression of TM9SF2 in wild-type HAP1 (middle) and mutant HAP1ΔTM9SF2 cells (right) was

(Continued on next page)

N-sulfate in HS. This assay revealed that the numbers of HS chains were similar in the HAP1ΔTM9SF2 cells, the rescued cells, and the wild-type HAP1 cells, whereas the amount of N-sulfate was very much reduced in the HAP1ΔTM9SF2 cells compared to their rescued cells and the wild-type HAP1 cells. This is consistent with the idea that TM9SF2 modulates the activity of NDST1 (Fig. 5E and F). We next examined the localization of NDST1 in these cells. NDST1-EGFP, which was shown to be functional because it restored the loss of HS expression in HAP1ΔNDST1 cells (data not shown), was clearly colocalized with GM130 in the wild-type and rescued cells, whereas the fluorescence intensity of NDST1-EGFP was significantly weaker in the HAP1ΔTM9SF2 cells, and some molecules localized to the Golgi, but some did not (Fig. 5G). This suggests that TM9SF2 is critical for the correct localization of NDST1 and that this mis-sorting causes the degradation of NDST1. To examine whether NDST1-EGFP was degraded in the HAP1ΔTM9SF2 cells, an NDST1-EGFP-IRES-BFP expression construct was stably introduced into the cells, and the expression of NDST1-EGFP was compared to the blue fluorescent protein (BFP) expression in each cell type. Flow cytometry clearly demonstrated that NDST1-EGFP expression was significantly lower in the HAP1ΔTM9SF2 cells when normalized to BFP (Fig. 5H), indicating that the stability of NDST1 was compromised in the HAP1ΔTM9SF2 cells. These results indicate that Golgi compartment-resident TM9SF2 is critical for the correct localization and stability of NDST1. Finally, to confirm the selective effect of defective TM9SF2 on NDST1 and HS expression in the context of viral infection, the susceptibilities of HAP1ΔTM9SF2 and HAP1ΔNDST1 cells to CHIKV (Thai#16856 strain), SINV, JEV, and YFV were examined (Fig. 5I). The decreased susceptibility of HAP1ΔTM9SF2 cells was only observed in CHIKV among four viruses compared to wild-type cells and showed a similar tendency compared to susceptibility of HAP1ΔNDST1 cells, although the resistances in HAP1ΔTM9SF2 cells were slightly milder than those in HAP1ΔNDST1 cells; this was most likely due to the incomplete inactivation of NDST1 function in HAP1ΔTM9SF2 cells. Thus, TM9SF2 is critical for CHIKV infection because it is specifically essential for normal NDST1 activity.

Enhanced infectivity by conversion of glycine 82 in E2 to arginine is not dependent on GAGs. Finally, we examined whether conversion of glycine 82 in E2 of Thai#16856 strain to arginine affects the infectivity to HAP1 derivative cells, because a Gly82-to-Arg conversion in a clinical isolate strongly enhanced the infectivity, which was dependent on the HS expression of the host cells, similarly to a vaccine strain (45). In fact, this conversion enhanced the infectivity of the Thai#16856 pseudovirus to rescued HAP1 cells of ΔNDST1 and ΔB3GAT3 (Fig. 6), as well as wild-type HAP1 cells

FIG 5 Legend (Continued)
analyzed by flow cytometry. The numbers indicate the G-MFIs. Wild-type HAP1 cells stained only with secondary antibody were used as the negative control (left). (D) Molecular sizes of glypican-3 in various HAP1-derived knockout and rescued cells. Cell lysates of these cells were subjected to immunoblotting to analyze the expression of glypican-3. (E) Analysis of N-sulfation and HS chain numbers in wild-type HAP1 (wild type+vector), TM9SF2-knockout cells (ΔTM9SF2+vector), and rescued TM9SF2-knockout cells (ΔTM9SF2+TM9SF2). Cells were incubated with or without 0.3 U of heparinase III at 37°C for 1 h and then stained with F58-10E4 (10E4) to detect HS expression and F69-3G10 (3G10) to determine HS chain numbers. Cells stained only with secondary antibody (Alexa 488-conjugated anti-mouse Ig or IgM antibody) were used as the negative control (without first antibody). Solid line, no enzyme treatment; dotted line, heparinase III treatment. (F) Quantitative analysis of the results in panel E. Relative ratios of cell surface N-sulfated HS (left columns), HS chain numbers (middle), and N-sulfates per HS chain (right) were calculated from the G-MFI values detected in panel E. The data represent the means ± the SE for three independent experiments. *, $P < 0.05$; **, $P < 0.01$. (G) Expression and intracellular localization of exogenously expressed EGFP-fused NDST1 (NDST1-EGFP) in wild-type HAP1 and HAP1ΔTM9SF2 cells. Cells stably expressing NDST1-EGFP were fixed and stained with anti-GM130 antibody. The pictures were taken under the same conditions. (H) Stability of NDST1-EGFP in HAP1ΔTM9SF2 cells. The construct shown in the upper panel, from which NDST1-EGFP and puro-T2A-BFP were cistronically transcribed, was stably integrated into wild-type HAP1, HAP1ΔNDST1, and HAP1ΔTM9SF2 cells. The stability of NDST1-EGFP was calculated as the ratio of EGFP intensity to the BFP intensity, which was measured by flow cytometry. The data represent the means ± the SD for two independent experiments. **, $P < 0.01$. (I) The susceptibilities of NDST1 and TM9SF2 knockout cells to CHIKV Thai#16856, SINV, JEV, and YFV were examined. The susceptibility of each cell is shown as the virus titer ($CCID_{50}$/50 μl). The data represent the means ± the SD for three independent experiments. Statistical significances between wild-type HAP1 and other HAP1 mutants or between mutant cell lines (showed on the horizontal bar) are indicated (*, $P < 0.05$; **, $P < 0.01$; ns, not significant).

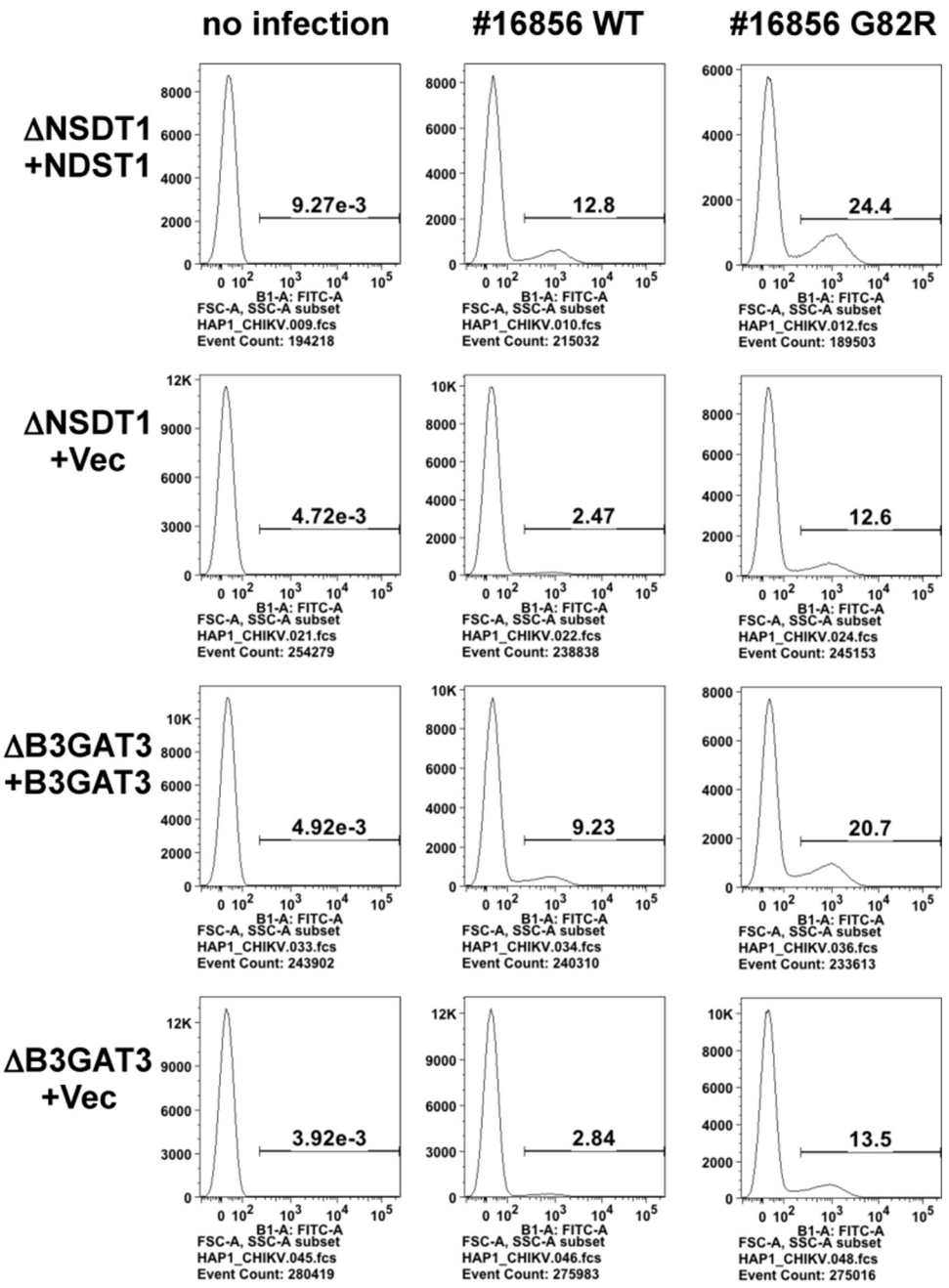

FIG 6 Enhanced infectivity by conversion of glycine 82 to arginine in CHIKV Thai#16856 pseudovirus. Totals of 10^5 HAP1ΔNDST1 and 10^5 HAP1ΔB3GAT3 rescued cells were inoculated for 2 h with 50 ng of p24-equivalent lentivirus-based pseudovirus bearing an EGFP gene as a reporter and wild-type CHIKV Thai#16856-E (Thai#16856 WT) or CHIKV Thai#16856-E3-1 G82R in which glycine 82 in E2 is converted to arginine (Thai#16856 G82R). The percentages of EGFP-positive cells were quantified by flow cytometry at 5 days after infection.

(data not shown). Surprisingly, this conversion also enhanced the infectivity to ΔNDST1 and ΔB3GAT3 HAP1 cells even stronger than the rescued cells, when Gly82Arg was compared to wild-type pseudovirus.

DISCUSSION

To identify the host factors involved in CHIKV infection in this study, we performed a genome-wide screening of a haploid human (HAP1) cell library randomly mutagenized with an insertional exon-trapping vector, combined with deep sequencing. This approach, which has recently been developed by Brummelkamp's group (25–27),

allowed us to identify many genes simultaneously in this study, not only as relevant (positive) candidates but also as irrelevant (negative) ones that were not enriched in the target cell population even though a significant number of exon-trapping vectors were inserted into the control cells. The genes were evaluated by comparing the numbers of different sites into which exon-trapping vectors were integrated in the target and control cell populations. However, this method requires that a significant number of exon-trapping vectors are inserted into genes of interest, and the genes that are not expressed in the cells or function redundantly with other gene(s) in a specific step cannot be evaluated.

With this excellent approach, our genome-wide screen suggested that several enzymes involved in HS biosynthesis are critical for CHIKV infection, whereas others are nonessential. This was confirmed by establishing knockout cell lines of individual genes with the CRISPR/Cas9 system. In this way, we established the minimum structure of HS that is essential for efficient CHIKV infection of HAP1 cells.

Because the envelope proteins E2 and E1 in the pseudotyped VSV we used for screening were the only proteins that originated from CHIKV, the host cell factors involved in the surface binding of the pseudotyped VSV, its entry, and its fusion with the endosomal membrane were considered to be relevant to CHIKV infection. The genes identified here encoded proteins that were classified into three categories: enzymes known to act in the HS biosynthetic pathway, nonenzymatic proteins previously reported to be involved in HS expression (27), and proteins whose relationships with the HS pathway are unknown. Notably, more than half the genes identified here were associated with HS biosynthesis and/or expression, indicating the importance of HS and the validity of our experiments, because HS is almost the only host receptor for CHIKV infection reported so far (45, 46). It is well known that cell surface GAGs are the primary attachment factors for many kinds of viruses (reviewed in reference 47). GAGs are unbranched, high-molecular-weight polysaccharides that contain repeating disaccharide units of *N*-acetylglucosamine (GlcNAc) and D-glucuronic acid (GlcA) in the HS backbone and disaccharide units of GalNAc and GlcA in the CS backbone. GAGs attach to specific sites on the core proteins, generating proteoglycans (48). These backbone disaccharides are decorated with many N and O sulfates, generating their most important characteristics of bearing negative charges, or epimerized, which converts GlcA to L-iduronic acid (IdoA). Thus, many structural variations are produced. Among the GAGs, HS is frequently relevant to the infection and virulence of viruses (49, 50), including several alphaviruses, such as eastern equine encephalitis virus (51), Ross River virus (23), Sindbis virus (35, 52), Semliki forest virus (53), and Venezuelan equine encephalitis virus (54). The interactions between cell-surface GAGs and viruses are partly attributable to nonspecific electrostatic interactions between the negative charge of GAGs and the basic amino acids of the viral envelope proteins but also to the binding between specific structures of the GAGs and viral proteins. This is exemplified by the requirement for the 3-O-sulfation of specific glucosamine residues of HS by herpes simplex virus type 1 (55–57), for N-sulfation-rich and IdoA-containing HS by respiratory syncytial virus (58), for N- and 6-O-sulfated but not 2-O-sulfated HS by hepatitis C virus and coxsackievirus B3 variant PD (59–61), for syndecan-1 bearing N- and 6-O-sulfated HS by baculovirus (62), and for predominantly syndecans via 6-O-sulfation by hepatitis E virus (63), which allow the entry of individual viruses into host cells. Hence, the specific structures of HS that are critical for the entry of several viruses have been analyzed, although these structures are still unknown for many viral infections, probably because HS is structurally complex. In the present study, we identified for the first time N-sulfated HS as the minimum structure required for efficient CHIKV binding and infection to HAP1 cells for the following reasons. First, genes encoding the enzymes that catalyze HS biosynthesis, such as *FAM20B*, *B3GAT3*, *EXTL3*, *EXT1*, *EXT2*, and *NDST1*, were identified as critical host factors, whereas no genes encoding proteins that act after the N-sulfation step, which is catalyzed by NDST1, were identified as enriched. In particular, *GLCE*, encoding the only enzyme that acts immediately downstream of NDST1 and catalyzes the C5 epimerization of GlcA to IdoA, was not enriched in the

target cells, even though a significant number of exon-trapping vectors were inserted into the control cells. This indicates that GLCE is not a critical molecule in CHIKV infection, which was confirmed in *GLCE*-knockout cells. Importantly, this step is essential for the subsequent downstream modifications of the 2-O and most likely 3-O-sulfation of HS, indicating that neither type of O-sulfation is required for efficient CHIKV infection. Second, although it has not been completely proven whether C5 epimerization is required for 3-O-sulfation, CHIKV efficiently infected CHO cells lacking 3-O-sulfation (45, 46), indicating that the 3-O-sulfation of HS is not essential for efficient CHIKV infection, supporting our conclusion. Third and finally, it has been reported that 6-O-sulfation occurs independently of N-sulfation to some extent (64, 65). If 6-O-sulfation without N-sulfation is critical for CHIKV infection, the knockout of *NDST1* would not prevent CHIKV infection, or *NDST1*-knockout cells would be more susceptible to infection than *B3GAT3*-knockout cells, in which all N- and O-sulfation are completely lost. However, no significant differences were observed between *NDST1*- and *B3GAT3*-knockout cells, indicating that like 2-O- and 3-O-sulfation, 6-O-sulfation is not significantly involved in CHIKV infection. Since not all of the evidence described above was derived from human cells, we cannot completely exclude the possibility that human HS pathway and enzyme specificities are different from those of other species.

It has been reported that clinical isolates and lab strains of CHIKV showed different preferences to GAGs. Lab strains that appeared by culture adaptation but not clinical isolates were dependent on HS for infection. CHIKV-LR, a clinical isolate, is almost entirely HS independent (51). Another clinical isolate, SL15649, readily infected cells that express excess CS but that are devoid of HS, whereas vaccine strain 181/25 did not (45). Concerning this point, we sequenced the authentic CHIKV Thai#16856 strain using a stocked aliquot of exactly the same lot that we used in our study and confirmed that our CHIKV strain, the Thai#16856 strain, has only one different amino acid (glutamine 252) from that of the CHIKV-LR strain (lysine 252; GenBank accession no. EU224268.1) in the E1/E2 sequence. This variation (Lys252 to Gln) eliminates a positive charge that is favorable for GAG binding and was observed in 32 CHIKV strains among 159 strains recorded in UniProt database (data not shown), most of which are clinical isolates. Thai#16856 strain have does not have a mutation of Gly82 to Arg of E2 (45) or any other amino acid substitutions that were reported in E2 at passages 5 and 10 after cell culture adaptation of CHIKV-LR (46). Thus, the Thai#16856 strain we used here was considered to be a clinical isolate. Therefore, our finding that the infection by a clinical Thai#16856 strain isolate of HAP1 cells was dependent on N-sulfated HS is inconsistent with previous results. The most reasonable explanation for this discrepancy is the difference in cells used; the earlier study used CHO-derived GAG mutants, and we used human HAP1-derived knockout cells for the CHIKV infection assay. The GAG backbones of various lengths are modified with N- and O-sulfation at various positions and to various extents and also subjected to isomerization of GlcA. Thus, GAG structures, even among HS or CS, are extremely diverse, especially among cell lines. This, taken together with the fact that the precise GAG structures affecting the CHIKV binding and proliferation have not been determined, suggests that different cell lines may exhibit different virus binding properties and proliferation through different GAG structures. Several mutations, including the Gly82Arg mutation of E2 observed in lab and vaccine strains, were considered to enhance binding to GAGs (45, 46). We examined whether Gly82Arg conversion in CHIKV Thai#16856 E2 also enhanced the infectivity to HAP1 cells. This conversion indeed enhanced the infectivity but, surprisingly, this enhancement was not dependent on GAGs because a similar enhancing effect was observed in HAP1ΔNDST1 and HAP1ΔB3GAT3 cells (Fig. 6). This result strongly demonstrates that the infection manner of CHIKV varies among the host cells and that different binding partners other than GAG may yield different preferences to GAGs. It is well known that many viruses, such as flaviviruses, use multiple molecules besides GAGs for the receptor and that the dependence of each receptor is specific to the host cell type (66, 67). Since CHIKV can still infect cells lacking GAGs, albeit with lower efficiency, CHIKV should use undefined receptors other than GAGs. Alternatively, the relatively low expression of CS on HAP1

cells could lead to a possibly biased result that N-sulfation is a strong determinant in HAP1 cells. CS is another GAG often associated with viral infection (68–74). Indeed, overexpression of CS on HAP1ΔNDST1 cells restored the 50% cell culture infectious dose ($CCID_{50}$) of the authentic CHIKV Thai#16856 strain, a finding consistent with a previous argument that the clinical isolate SL15649 readily infected CHO mutant cells that express excess CS (45). Nevertheless, this did not recover the infectivity of pseudovirus and binding of authentic virions to cells (Fig. 3), indicating that CS plays a role at later steps after the CHIKV binding and entry to the HAP1 cells. Kim et al. reported that soluble CS-E (sCS-E), a form of CS composed of GlcA-GalNAc(4,6-O-disulfate) but not other types of CS (CS-A, -B, -C, and -D and heparin) significantly enhanced JEV infection in the mouse neuroblastoma cell line Neuro-2a and in a rat infection model, probably through the increased viral RNA replication, although viral attachment to Neuro-2a cells was inhibited by sCS-E (75). These researchers also demonstrated that sCS-E inhibited not only JEV attachment to Vero and BHK cells similar to Neuro-2a cells but also JEV infection of these cell lines in contrast to Neuro-2a, indicating that the sCS-E effect is cell type specific (75). These evidences are consistent with our ideas that CS plays a role at later steps after CHIKV binding and entry into HAP1 cells and that the manner of utilizing GAGs is cell type specific, although the mechanisms remain to be clarified.

We identified the genes which did not encode enzymes that catalyze HS biosynthesis as candidates involved in CHIKV entry. Among these genes encoding nonenzymatic proteins, the *COG* family, *TMEM165*, *TM9SF2*, *PTAR1*, *SLC39A9*, and *SACM1L* have been shown to be associated with N-sulfated HS expression by a haploid genetic genome-wide screening, although Jae et al. did not confirm whether the defects in these genes truly affected the expression of N-sulfated HS (27). We confirmed this with flow cytometry by measuring the surface expression of N-sulfated HS on cells in which the individual genes were knocked out (except *SACM1L*, because we failed to establish the knockout cells). To our knowledge, among these genes, only defects in *TMEM165* and *PTAR1* have been previously shown to reduce surface HS expression (33, 76). Moreover, we newly demonstrated that *TM9SF2*-, *PTAR1*-, and *SLC39A9*-knockout cells, as well as *COG7*- and *TMEM165*-knockout cells, displayed abnormalities in multiple glycosylation pathways, to various extents. This is consistent with their localization to the Golgi apparatus (our unpublished observations), where these glycosylations occur. This raises the possibility that the impaired glycosylation of molecules other than GAG, such as sialylation, another major source of negative charges, might affect the binding and infectivity of CHIKV similar to the impaired sulfation of HS, as shown in previous report (77). This possibility would explain why SLC39A9, whose defect only weakly affected the expression of N-sulfated HS, was identified as a candidate gene. The knockout of *TM9SF2* had a relatively strong and selective effect on HS expression, so we analyzed the mechanisms by which HS expression is impaired by defective TM9SF2. Members of the TM9 superfamily are well conserved among all types of eukaryotes, and in mammals four proteins (TM9SF1 to TM9SF4) belong to this superfamily. It has recently been reported that the TM9SF proteins in yeast and plant homologues localize to the Golgi compartment (78), an observation consistent with our results, and are implicated in the homeostasis of metals, such as copper (79). Because (metal) ion homeostasis is critical for Golgi body function, as shown by defects in TMEM165 and GPHR (Golgi pH regulator) (32, 80), and because impaired ion homeostasis is known to cause the mis-sorting and degradation of Golgi proteins (39), this putative function reasonably explains the mislocalization and degradation of NDST1 caused by the knockout of *TM9SF2*, although a more detailed analysis is still required.

Here, we report that N-sulfated HS is the minimum structure essential for the efficient binding and infection of HAP1 cells by CHIKV and that CS plays roles at later steps after CHIKV binding and entry into the HAP1 cells, and we identified genes involved in the expression of N-sulfated HS using haploid genetic genome-wide screening of cell susceptibility to a CHIKV pseudovirus. Although important issues remain to be resolved, such as whether these conclusions are applicable to different clinical CHIKV

strains and host mammalian cells other than those used here, the information presented here contributes to our understanding of CHIKV propagation, cell tropism, and pathogenesis and may contribute to the development of therapies to reduce the CHIKV load in infected carriers.

MATERIALS AND METHODS

Cells and viruses. HAP1 cells (81) and the derived mutant cell lines were grown in Iscove modified Dulbecco medium supplemented with 10 or 15% (vol/vol) fetal bovine serum (FBS), 50 U/ml penicillin, and 50 μg/ml streptomycin. 293T cells and HEK293 cells were grown in Dulbecco modified Eagle medium supplemented with 10% (vol/vol) FBS, 50 U/ml penicillin, and 50 μg/ml streptomycin. Vero and BHK cells were grown in Eagle minimum essential medium supplemented with 10% (vol/vol) FBS, 50 U/ml penicillin, and 50 μg/ml streptomycin. CHIKV strains were used in this study; Ross strain (GenBank accession no. AF490259) was first isolated in Tanzania by Ross during an outbreak in 1953 (34, 82), and the Thai#16856 strains were isolated in Thailand in 2009 (83). These CHIKV strains and Sindbis virus (SINV) Ar-339 strain (84) were propagated in BHK cells. Japanese encephalitis virus (JEV) JaGAr strain (85) and yellow fever virus (YFV) 17D vaccine strain (86) were propagated in Vero cells. Studies using CHIKV were conducted in a biosafety level 3 laboratory at RCC-ERI in Thailand with protocols approved by the institutional review boards of the National Institute of Health, Thailand, and Osaka University, Japan.

Plasmids, antibodies, and enzymes. Genomic RNAs of CHIKV Ross and Thai#16856 strains were extracted by using a QIAamp viral RNA minikit (Qiagen, Hilden, Germany). First-strand cDNA was synthesized using a SuperScript III reverse transcriptase kit (Invitrogen Corp., Carlsbad, CA) with a poly(dT)20+NotI+XbaI primer (5′-AAATCTAGAGCGGCCGCTTTTTTTTTTTTTTTTTT-3′). The structural gene, E3-E2-6k-E1 of CHIKV (Ross or Thai#16856 strain), was amplified by PCR from the first-strand cDNA using the sense primer SacI-ATG-signalseq-CHIKV-E3 (AAAGAGCTCATGAGTCTTGCCATC) and the antisense primer NheI-CHIKV-E1-Rev (AGCTGCTAGCTTAGTGCCTGCTGAACGACACGCATAGCACCACGA) and was cloned into SacI and NheI sites of the mammalian expression plasmid pCAGGS (pCAGGS/E3-E1). The exon-trapping vector, pPB-SA-pgkPur, was constructed as follows. First, pPB-SAIRES-BSD2 was made by subcloning of NheI-BamHI fragment coding IRES-BSD from pCMT-SAIRES-BSDpA (a gift from K. Horie) (87) into SpeI- and BamHI-digested pPB-SA hyg NP21 pA (kindly provided by the Wellcome Trust Sanger Institute, Cambridge, United Kingdom) (29). Then, the IRES-BSD portion of pPB-SAIRES-BSD2 was replaced with pgkPur, a PGK promoter-driven puromycin-resistant gene, yielding pPB-SA-pgkPur. pX330-EGFP vector was constructed by insertion of cDNA fragment encoding enhanced green fluorescent protein (EGFP) into the FseI site within the nuclear localization signal at the C terminus of *Streptococcus pyogenes* Cas9 in pX330-U6-Chimeric_BB-CBh-hSpCas9 (plasmid 42230; Addgene, Cambridge, MA). EST clones (BC130293, BC071961, BC066098, and BC094587 for human TM9SF2, human B3GAT3, mouse NDST1, and mouse GLCE, respectively) were commercially purchased. Other cDNAs were amplified by reverse transcription-PCR (RT-PCR) from HAP1 RNA. The sequences of the PCR primers for the CSGALNACT1, COG7, PTAR1, SLC39A9, and TMEM165 genes are as follows: CSGALNACT1/sense (5′-CCTGCAGGCCTCGAGACCATGATGATGGTTCGCCGGG-3′) and CSGALNACT1/antisense (5′-ATTTACGTAGCGGCCGCTATGTTTTTTTGCTACTTGTCTTCTGTTTCTG-3′) (GenBank accession no. NM_001130518.1); hCOG7/sense (5′-TCCTGCAGGCCTCGAGTCGACGCCATGGACTTCTCCAAGTT-3′) and hCOG7/antisense (5′-ATTTACGTAGCGGCCGCTCAGTAATTCACACTCCGCATGGT-3′) (GenBank accession no. NM_153603.3); hPTAR1/sense (5′-ATTAAGGCCTGTCGACATGGCCGAGACCAGCGA-3′) and hPTAR1/antisense (5′-GGGGCCGAGGCGGCCGCACCTCTTTCATTGACTCAAAGTAACCAGC-3′) (GenBank accession no. NM_001099666.1); hSLC39A9/sense (5′-ATTAAGGCCTGTCGACATGGATGATTTCATCTCCATTAGCCTG-3′) and hSLC39A9/antisense (5′-GGGGCCGAGGCGGCCGCTTGAACATTTAATGCTGGTGTCCTACTG-3′) (GenBank accession no. NM_018375.4); and hTMEM165/sense (5′-TCCTGCAGGCCTCGAGTCGACATGGCAGCAGCGGCTCCAGGGAACG-3′) and hTMEM165/antisense (5′-ATTTACGTAGCGGCCGCTAAAAACCAGAATCAGGGCTTATAAATAGTGC-3′) (GenBank accession no. NM_018475.4). The initiation and termination codons are underlined. Each cDNA PCR products was cloned into the retroviral expression vector plasmid pMXs-IP (88) or pLIB-pgkPur, which was constructed by subcloning pgkPur downstream of the multicloning site of the pLIB vector (Clontech, Mountain View, CA).

Anti-CHIKV mouse MAb clone 29 against the CHIKV-E2 protein developed in our lab was used to detect virus particles bound to target cells. The mouse MAb clones used here were as follows: F58-10E4 against HS (US Biologicals, Salem, MA), CS56 against chondroitin sulfate (CS; Abcam, Cambridge, United Kingdom), 1G12 against glypican-3 (Santa Cruz Biotechnology, Santa Cruz, CA), MI15 against syndecan-1 (BioLegend, San Jose, CA), and F69-3G10 against delta HS and clone 35 anti-GM130 (BD Biosciences, San Jose, CA). Fluorescent dye-conjugated lectins and cholera toxin B subunit were purchased from Life Technologies (Carlsbad, CA). Heparinase III (EC 4.2.2.8) from *Flavobacterium heparinum* was purchased from Sigma (St. Louis, MO).

Preparation of pseudoviruses. VSVΔG*-G or VSVΔG-luci-G represents recombinant viruses composed of VSVΔG* or VSVΔG-luci, whose intrinsic envelope G gene was replaced with GFP (ΔG*) or luciferase gene (ΔG-luci), and whose envelope G protein (-G) was exogenously supplied. Because VSVΔG*-G and VSVΔG-luci-G recombinant viruses lacking VSV G gene cannot replicate by themselves, they were amplified by inoculation into 293T cells that had been transfected with pCAGGS/VSVG, an expression plasmid of VSV G protein (89, 90). CHIKV pseudoviruses, VSVΔG*-CHIKV-E (Ross strain) and VSVΔG-luci-CHIKV-E (Ross strain or Thai#16856 strain) bearing CHIKV E2/E1 proteins, were prepared by the inoculation of VSVΔG*-G and VSVΔG-luci-G, respectively, into 293T cells that had been transfected with pCAGGS/E3-E1, an expression plasmid of CHIKV envelope proteins E1 to E3. Two hours after the

incubation for viral adsorption, the cells were extensively washed with medium, and then medium supplemented with 2% FBS and 10 mM HEPES (pH 7.0) was added. Culture supernatants containing propagated VSVΔG*-CHIKV-E or VSVΔG-luci-CHIKV-E were harvested after 18 to 24 h of incubation at 37°C in a CO_2 incubator and clarified by low-speed centrifugation, and aliquots of the supernatants were stored at −80°C until use. The infectivity of VSVΔG-luci-CHIKV-E was assessed by measuring the luciferase activities within cells after incubation with VSVΔG-luci-CHIKV-E for 20 to 24 h using a Steady-Glo luciferase assay system (Promega Corporation, Madison, WI) according to the manufacturer's protocol.

Establishment of HAP1 mutant cell library using exon-trapping vector. A HAP1 mutant cell library was constructed by transfecting the *piggyback*-transposon-based exon-trapping vector pPB-SA-pgkPur and the transposase expression vector pCMV-hyPBase into 8×10^8 HAP1 cell by electroporation, resulting in an insertional mutant library with a complexity of about 10^8 independent clones after selection in 0.5 to 1.0 μg/ml puromycin.

Genome-wide screening with a next generation sequencer. A total of 1.4 billion HAP1 insertional mutant library cells were plated on 24 large plates and challenged with three rounds of inoculation with VSVΔG*-CHIKV-E (Ross strain) (MOI = 2.5 to 3) at 3-day intervals, which concentrated the target cell population. HAP1 insertional mutant library cells that were not infected with VSVΔG*-CHIKV-E were used as the control cell population. Subsequently, insertion sites of exon-trapping vector were decided by amplifying the genomic DNA adjacent to the inserted exon-trapping vectors using the splinkerette-PCR method (91). To explain briefly, genomic DNAs extracted from both target and control cell population were sonicated to produce 800-bp DNA fragments. Fragmented DNAs were blunt ended with dideoxynucleoside triphosphate, phosphorylated at the 5′ end, and ligated with a splinkerette adaptor made by preannealing of two oligonucleotides, Spl-L (5′-GGTCGATCTTCACGGTTTCTGCTACACTGTGGACTCCAACG AAGCGAAGG-3′) and Spl-S2 (5′-CCTTCGCTTCGTTGTTTTTTTTTTTGGGGAAAAAAAAAA-3′). To amplify the adjacent genomic DNAs, first-round PCR was carried out with Spl-F1 linker primer (5′-GGTCGATCTTCACGG TTTCTGC-3′) and PB3-1.5 exon-trapping vector primer (5′-TCAATTTTACGCATGATTATCTTTAACG-3′). The products were purified with Amicon Ultra filter and subjected to the second-round PCR using splinkerette Spl-F3 (5′-GTGACTGGAGTTCAGACGTGTGCTCTTCCGATCTGTGGACTCCAACGAAGCGAAGG-3′) and PB3-2 (5′-CGTACGTCACAATATGATTATCTTTCTAGGGT-3′). The second-round PCR products after size selection were subjected to deep sequencing (Illumina MiSeq) and analyzed using CLC Genomic Workbench software (Qiagen) as previously reported (92). The number of different sites at which the exon-trapping vector had inserted was determined in each gene. By comparing the numbers in the target cells to those in the control cells, we selected the genes in the target cell population with significantly increased numbers of insertion sites (FDR < 0.05) as the enriched candidate genes.

Establishment of knockout cells and its knock-in rescued cells. Target gene knockout cells were established by transfection of pX330-EGFP vector with a target guide RNA sequence into HAP1 cells. The sequences of the guide RNAs were as follows: *B3GAT3*, GTGTGTGAAGAGGAGGCCAG and GTTCCGCTGC TCGACACCAC; *NDST1*, GTGGAGAAAGGTGTGCTCCC and GTGCAGTGCAGCATGCAGGC; *GLCE*, GTCTGAGG AAGCATTCCCTC and GAGCCCCCTATCACCCCGA; *COG7*, GGCAGACGACTTCGACGTGA and ACAGCTGCA GCTTCATCACC; *TMEM165*, GCCAAATTAGTTTGGGTAGC and GTTATAGCGCATTGCCATGA; *PTAR1*, GAACCA GGACTATGGGACTC and ACAAACTGGGTGTGGAGAGC; *SLC39A9*, ATGCAGCTGTGTGTGGTCG and ATTGGT GTTTCCCTCGTTC; *TM9SF2*, AACCACTGAATGTGGGTATG. Three to four days after transfection of the targeting vector, HAP1 cells expressing EGFP were collected by a cell sorter. A couple of days after cell sorting, the sorted cells were plated into 96-well multiplate for limiting dilution. Cloned cells were verified by sequencing to determine whether suitable genomic editing occurred in the target gene (data not shown).

Virus infections. To examine the susceptibilities of cells to the wild-type CHIKV, SINV, JEV, and YFV, the target cells were plated into 96-well multiplates 1 to 2 days before inoculation, and then serially diluted virus solutions were inoculated. Cell viability in each well was measured by using the cell proliferation reagent WST-1 (Roche Applied Sciences, Germany) according to the manufacturer's protocol 3 to 4 days after incubation. Virus infection was regarded as positive when the WST value of each well was decreased by $> 25\%$ compared to that of an uninoculated cell well. Values for $CCID_{50}$/50 μl were calculated using the Reed-Muench calculation. The WST-LD_{50} was defined as the dilution of virus showing half of the maximum WST values estimated by a logistic equation that was calculated from the WST values by logistic regression using the maximum-likelihood method (Fig. 2D, 3D, 4D, and 5I). Statistical analysis using $CCID_{50}$/50 μl and WST-LD_{50} yielded very similar results (data not shown); therefore, only the values for $CCID_{50}$/50 μl are reported here. After we measured the WST values, the cells were stained with crystal violet after fixation by phosphate-buffered saline (PBS) containing 3.7% formaldehyde.

To examine the susceptibilities of cells to VSVΔG*-CHIKV-E and VSVΔG-luci-CHIKV-E, the target cells were plated into 96-well plates (2×10^4 cells/well) 1 to 2 days prior to inoculation. Serially diluted pseudotyped VSVs were inoculated into the cell culture, and 1 day after the inoculation the luciferase activity was measured using a Steady-Glo luciferase assay system.

CHIKV binding assay. The culture medium was replaced with a fresh one for subconfluent target cells plated into 96-well plates before virus inoculation. The CHIKV Thai#16856 strain purified by cesium chloride density gradient ultracentrifugation was added to the culture medium, followed by incubation for 1 h at 4°C. The cells were washed twice with culture medium and fixed using 2% paraformaldehyde for 1 h. After fixation, the cells were washed twice with water, treated with anti-CHIKV mouse MAb (2.5 μg/ml in PBS containing 5% skim milk) for 30 min at room temperature, washed four times with PBS, and then added to SureBlue TMB Microwell peroxidase substrate (Kirkegaard & Perry Laboratories, Inc., Gaithersburg, MD) at 100 μl/well. The plate was incubated for 13 to 15 min at room temperature in the

dark. A reaction stop solution (0.6 N sulfuric acid) was added to each well (100 μl/well), and the optical density at 450 nm (OD_{450}) and OD_{620} were measured with a Multiskan FC microplate photometer (Thermo Scientific, Rockford, IL).

Development of chicken IgY against human TM9SF2. A cDNA region encoding amino acids 29 to 300 of human *TM9SF2* was amplified by PCR using an EST clone (BC130293) as a template DNA and the primers EK-HRV3C-TM9SF2F (GATGACGATGACAAAGGCCTGGAAGTGCTGTTCCAAGGCCCGCGCCGGA) and TM9SF2-breviR2 (CATCCTGTTAAGCTTACGCGTTCACTGAATGTGGGTATGAGGCATAGA). The PCR fragment was subcloned into *Brevibacillus* expression vector pBIC3 (TaKaRa Shuzo Co., Ltd., Ohtsu, Shiga, Japan). The resulting pBIC3-HRV3C-hTM9SF2(29–300) was transformed into *Brevibacillus choshinensis* competent cells (TaKaRa Shuzo Co., Ltd., Shiga, Japan). Recombinant protein was produced according to the manufacturer's protocol and purified according to the following steps: precipitation with ammonium sulfate (60% saturation), dialysis against buffer A (50 mM Tris-HCl [pH 8.0], 0.5 M NaCl, and 15% glycerol), affinity purification by Ni-NTA resin column (Qiagen), elution with 250 mM imidazole in buffer A, digestion with PreScission (GE Healthcare, Little Chalfont, Buckinghamshire, United Kingdom), dialysis against buffer A with 14 mM 2-mercaptoethanol, and the removal of PreScission and the N-terminal His tag region using Ni-NTA and glutathione columns. Chickens were inoculated five times with purified recombinant protein. Eggs from the immunized chickens were collected, and the IgY fractions were purified using polyethylene glycol 6000.

Flow cytometric analysis. To examine the cell surface expression of various glycans, 10^6 cells per sample were harvested from tissue culture dishes using PBS supplemented with 2.5 mM EDTA and 0.1% bovine serum albumin. These cells were then stained with antibodies or fluorescent dye-conjugated lectins suspended in 50 μl of PBS containing 3% bovine serum albumin and 0.1% sodium azide according to the standard protocol and analyzed using a flow cytometer (MACSQuant; Miltenyi Biotech GmbH, Bergisch Gladbach, Germany) as previously reported (80).

Accession number(s). The raw Illumine data set has been deposited in the DDBJ Sequence Read Archive (accession number DRA005263; BioProject PRJDB5298). The read counts in the control and target cell populations of all genes identified here and their significances are reported in Data Set S1 in the supplemental material.

SUPPLEMENTAL MATERIAL

Supplemental material for this article may be found at https://doi.org/10.1128/JVI.00432-17.

SUPPLEMENTAL FILE 1, XLSX file, 0.9 MB.

ACKNOWLEDGMENTS

We thank T. R. Brummelkamp and the Whitehead Institute for Biomedical Research for the HAP1 cells; J. Takeda (Medical School, Osaka University), K. Horie (Medical School, Osaka University), and K. Yusa, and the Wellcome Trust Sanger Institute for the pCMT-SAIRES-BSDpA, pPB-SA hyg NP21 pA, and pCMV-hyPBase plasmids; T. Shiota (Department of Viral Infection, Research Institute for Microbial Diseases [RIMD]) for the SINV strain; Y. Matsuura (Department of Viral Infection, RIMD) for the recombinant VSVs (VSVΔG*-G and VSVΔG-luci-G) and the pCAGGS/VSVG plasmid; Kohjiro Nakamura and Yuko Kabumoto for assistance with cell sorting; and Keiko Kinoshita and Yukari Hirata for technical help. We also thank the laboratory members of the Department of Immunoregulation, RIMD, Osaka University, Osaka, Japan, and of RCC-ERI, Thailand, for fruitful discussions and generous help.

This study was supported, in part, by grants-in-aid from the Japanese Society for the Promotion of Science and in part by the Japan Initiative for Global Research Network on Infectious Diseases (J-GRID) from the Ministry of Education, Culture, Sport, Science, and Technology of Japan and the Japan Agency for Medical Research and Development (AMED).

REFERENCES

1. Burt FJ, Rolph MS, Rulli NE, Mahalingam S, Heise MT. 2012. Chikungunya: a re-emerging virus. Lancet 379:662–671. https://doi.org/10.1016/S0140-6736(11)60281-X.
2. Brouard C, Bernillon P, Quatresous I, Pillonel J, Assal A, De Valk H, Desenclos JC; Quantitative Estimation of the Risk of Blood Donation Contamination by Infectious Agents Workgroup. 2008. Estimated risk of Chikungunya viremic blood donation during an epidemic on Reunion Island in the Indian Ocean, 2005 to 2007. Transfusion 48:1333–1341. https://doi.org/10.1111/j.1537-2995.2008.01646.x.
3. Pialoux G, Gauzere BA, Jaureguiberry S, Strobel M. 2007. Chikungunya, an epidemic arbovirosis. Lancet Infect Dis 7:319–327. https://doi.org/10.1016/S1473-3099(07)70107-X.
4. Mavalankar D, Shastri P, Raman P. 2007. Chikungunya epidemic in India: a major public-health disaster. Lancet Infect Dis 7:306–307. https://doi.org/10.1016/S1473-3099(07)70091-9.
5. Schwartz O, Albert ML. 2010. Biology and pathogenesis of chikungunya virus. Nat Rev Microbiol 8:491–500. https://doi.org/10.1038/nrmicro2368.
6. Chua KB. 2010. Epidemiology of chikungunya in Malaysia: 2006-2009. Med J Malaysia 65:277–282.
7. Pulmanausahakul R, Roytrakul S, Auewarakul P, Smith DR. 2011. Chikun-

gunya in Southeast Asia: understanding the emergence and finding solutions. Int J Infect Dis 15:e671–6. https://doi.org/10.1016/j.ijid.2011.06.002.
8. Sam IC, Loong SK, Michael JC, Chua CL, Wan Sulaiman WY, Vythilingam I, Chan SY, Chiam CW, Yeong YS, AbuBakar S, Chan YF. 2012. Genotypic and phenotypic characterization of Chikungunya virus of different genotypes from Malaysia. PLoS One 7:e50476. https://doi.org/10.1371/journal.pone.0050476.
9. Pongsiri P, Auksornkitti V, Theamboonlers A, Luplertlop N, Rianthavorn P, Poovorawan Y. 2010. Entire genome characterization of Chikungunya virus from the 2008-2009 outbreaks in Thailand. Trop Biomed 27:167–176.
10. Weaver SC. 2014. Arrival of chikungunya virus in the new world: prospects for spread and impact on public health. PLoS Negl Trop Dis 8:e2921. https://doi.org/10.1371/journal.pntd.0002921.
11. Morrison TE. 2014. Reemergence of chikungunya virus. J Virol 88:11644–11647. https://doi.org/10.1128/JVI.01432-14.
12. Parola P, de Lamballerie X, Jourdan J, Rovery C, Vaillant V, Minodier P, Brouqui P, Flahault A, Raoult D, Charrel RN. 2006. Novel chikungunya virus variant in travelers returning from Indian Ocean islands. Emerg Infect Dis 12:1493–1499. https://doi.org/10.3201/eid1210.060610.
13. Schuffenecker I, Iteman I, Michault A, Murri S, Frangeul L, Vaney MC, Lavenir R, Pardigon N, Reynes JM, Pettinelli F, Biscornet L, Diancourt L, Michel S, Duquerroy S, Guigon G, Frenkiel MP, Brehin AC, Cubito N, Despres P, Kunst F, Rey FA, Zeller H, Brisse S. 2006. Genome microevolution of chikungunya viruses causing the Indian Ocean outbreak. PLoS Med 3:e263. https://doi.org/10.1371/journal.pmed.0030263.
14. Simizu B, Yamamoto K, Hashimoto K, Ogata T. 1984. Structural proteins of Chikungunya virus. J Virol 51:254–258.
15. Jose J, Snyder JE, Kuhn RJ. 2009. A structural and functional perspective of alphavirus replication and assembly. Future Microbiol 4:837–856. https://doi.org/10.2217/fmb.09.59.
16. Leung JY, Ng MM, Chu JJ. 2011. Replication of alphaviruses: a review on the entry process of alphaviruses into cells. Adv Virol 2011:249640. https://doi.org/10.1155/2011/249640.
17. Voss JE, Vaney MC, Duquerroy S, Vonrhein C, Girard-Blanc C, Crublet E, Thompson A, Bricogne G, Rey FA. 2010. Glycoprotein organization of Chikungunya virus particles revealed by X-ray crystallography. Nature 468:709–712. https://doi.org/10.1038/nature09555.
18. Kielian M. 2010. Structural biology: An alphavirus puzzle solved. Nature 468:645–646. https://doi.org/10.1038/468645a.
19. Zhang W, Heil M, Kuhn RJ, Baker TS. 2005. Heparin binding sites on Ross River virus revealed by electron cryo-microscopy. Virology 332:511–518. https://doi.org/10.1016/j.virol.2004.11.043.
20. Sanz MA, Rejas MT, Carrasco L. 2003. Individual expression of Sindbis virus glycoproteins. E1 alone promotes cell fusion. Virology 305:463–472.
21. Omar A, Koblet H. 1988. Semliki Forest virus particles containing only the E1 envelope glycoprotein are infectious and can induce cell-cell fusion. Virology 166:17–23. https://doi.org/10.1016/0042-6822(88)90141-9.
22. Justman J, Klimjack MR, Kielian M. 1993. Role of spike protein conformational changes in fusion of Semliki Forest virus. J Virol 67:7597–7607.
23. Heil ML, Albee A, Strauss JH, Kuhn RJ. 2001. An amino acid substitution in the coding region of the E2 glycoprotein adapts Ross River virus to utilize heparan sulfate as an attachment moiety. J Virol 75:6303–6309. https://doi.org/10.1128/JVI.75.14.6303-6309.2001.
24. Carette JE, Guimaraes CP, Wuethrich I, Blomen VA, Varadarajan M, Sun C, Bell G, Yuan B, Muellner MK, Nijman SM, Ploegh HL, Brummelkamp TR. 2011. Global gene disruption in human cells to assign genes to phenotypes by deep sequencing. Nat Biotechnol 29:542–546. https://doi.org/10.1038/nbt.1857.
25. Carette JE, Raaben M, Wong AC, Herbert AS, Obernosterer G, Mulherkar N, Kuehne AI, Kranzusch PJ, Griffin AM, Ruthel G, Dal Cin P, Dye JM, Whelan SP, Chandran K, Brummelkamp TR. 2011. Ebola virus entry requires the cholesterol transporter Niemann-Pick C1. Nature 477:340–343. https://doi.org/10.1038/nature10348.
26. Jae LT, Raaben M, Herbert AS, Kuehne AI, Wirchnianski AS, Soh TK, Stubbs SH, Janssen H, Damme M, Saftig P, Whelan SP, Dye JM, Brummelkamp TR. 2014. Virus entry: Lassa virus entry requires a trigger-induced receptor switch. Science 344:1506–1510. https://doi.org/10.1126/science.1252480.
27. Jae LT, Raaben M, Riemersma M, van Beusekom E, Blomen VA, Velds A, Kerkhoven RM, Carette JE, Topaloglu H, Meinecke P, Wessels MW, Lefeber DJ, Whelan SP, van Bokhoven H, Brummelkamp TR. 2013. Deciphering the glycosylome of dystroglycanopathies using haploid screens for Lassa virus entry. Science 340:479–483. https://doi.org/10.1126/science.1233675.
28. Rosmarin DM, Carette JE, Olive AJ, Starnbach MN, Brummelkamp TR, Ploegh HL. 2012. Attachment of *Chlamydia trachomatis* L2 to host cells requires sulfation. Proc Natl Acad Sci U S A 109:10059–10064. https://doi.org/10.1073/pnas.1120244109.
29. Yusa K, Zhou L, Li MA, Bradley A, Craig NL. 2011. A hyperactive *piggyBac* transposase for mammalian applications. Proc Natl Acad Sci U S A 108:1531–1536. https://doi.org/10.1073/pnas.1008322108.
30. Zeevaert R, Foulquier F, Jaeken J, Matthijs G. 2008. Deficiencies in subunits of the conserved oligomeric Golgi (COG) complex define a novel group of congenital disorders of glycosylation. Mol Genet Metab 93:15–21. https://doi.org/10.1016/j.ymgme.2007.10.019.
31. Wu X, Steet RA, Bohorov O, Bakker J, Newell J, Krieger M, Spaapen L, Kornfeld S, Freeze HH. 2004. Mutation of the COG complex subunit gene COG7 causes a lethal congenital disorder. Nat Med 10:518–523. https://doi.org/10.1038/nm1041.
32. Foulquier F, Amyere M, Jaeken J, Zeevaert R, Schollen E, Race V, Bammens R, Morelle W, Rosnoblet C, Legrand D, Demaegd D, Buist N, Cheillan D, Guffon N, Morsomme P, Annaert W, Freeze HH, Van Schaftingen E, Vikkula M, Matthijs G. 2012. TMEM165 deficiency causes a congenital disorder of glycosylation. Am J Hum Genet 91:15–26. https://doi.org/10.1016/j.ajhg.2012.05.002.
33. Dulary E, Potelle S, Legrand D, Foulquier F. 2016. TMEM165 deficiencies in congenital disorders of glycosylation type II (CDG-II): clues and evidences for roles of the protein in Golgi functions and ion homeostasis. Tissue Cell 49(Pt A):150–156. https://doi.org/10.1016/j.tice.2016.06.006.
34. Ross RW. 1956. The Newala epidemic. III. The virus: isolation, pathogenic properties and relationship to the epidemic. J Hyg (Lond) 54:177–191.
35. Byrnes AP, Griffin DE. 1998. Binding of Sindbis virus to cell surface heparan sulfate. J Virol 72:7349–7356.
36. Lee E, Lobigs M. 2002. Mechanism of virulence attenuation of glycosaminoglycan-binding variants of Japanese encephalitis virus and Murray Valley encephalitis virus. J Virol 76:4901–4911. https://doi.org/10.1128/JVI.76.10.4901-4911.2002.
37. Lee E, Lobigs M. 2008. E protein domain III determinants of yellow fever virus 17D vaccine strain enhance binding to glycosaminoglycans, impede virus spread, and attenuate virulence. J Virol 82:6024–6033. https://doi.org/10.1128/JVI.02509-07.
38. Willett R, Kudlyk T, Pokrovskaya I, Schonherr R, Ungar D, Duden R, Lupashin V. 2013. COG complexes form spatial landmarks for distinct SNARE complexes. Nat Commun 4:1553. https://doi.org/10.1038/ncomms2535.
39. Demaegd D, Foulquier F, Colinet AS, Gremillon L, Legrand D, Mariot P, Peiter E, Van Schaftingen E, Matthijs G, Morsomme P. 2013. Newly characterized Golgi-localized family of proteins is involved in calcium and pH homeostasis in yeast and human cells. Proc Natl Acad Sci U S A 110:6859–6864. https://doi.org/10.1073/pnas.1219871110.
40. Aman AT, Fraser S, Merritt EA, Rodigherio C, Kenny M, Ahn M, Hol WG, Williams NA, Lencer WI, Hirst TR. 2001. A mutant cholera toxin B subunit that binds GM1-ganglioside but lacks immunomodulatory or toxic activity. Proc Natl Acad Sci U S A 98:8536–8541. https://doi.org/10.1073/pnas.161273098.
41. Rambaruth ND, Greenwell P, Dwek MV. 2012. The lectin Helix pomatia agglutinin recognizes O-GlcNAc containing glycoproteins in human breast cancer. Glycobiology 22:839–848. https://doi.org/10.1093/glycob/cws051.
42. Mandal DK, Nieves E, Bhattacharyya L, Orr GA, Roboz J, Yu QT, Brewer CF. 1994. Purification and characterization of three isolectins of soybean agglutinin: evidence for C-terminal truncation by electrospray ionization mass spectrometry. Eur J Biochem 221:547–553.
43. Swamy MJ, Gupta D, Mahanta SK, Surolia A. 1991. Further characterization of the saccharide specificity of peanut (*Arachis hypogaea*) agglutinin. Carbohydr Res 213:59–67. https://doi.org/10.1016/S0008-6215(00)90598-6.
44. Yang DH, Tsuyama S, Hotta K, Katsuyama T, Murata F. 2000. Expression of *N*-acetylglucosamine residues in developing rat fundic gland cells. Histochem J 32:187–193. https://doi.org/10.1023/A:1004051408239.
45. Silva LA, Khomandiak S, Ashbrook AW, Weller R, Heise MT, Morrison TE, Dermody TS. 2014. A single-amino-acid polymorphism in Chikungunya virus E2 glycoprotein influences glycosaminoglycan utilization. J Virol 88:2385–2397. https://doi.org/10.1128/JVI.03116-13.
46. Gardner CL, Hritz J, Sun C, Vanlandingham DL, Song TY, Ghedin E, Higgs S, Klimstra WB, Ryman KD. 2014. Deliberate attenuation of chikungunya virus by adaptation to heparan sulfate-dependent infectivity: a model

for rational arboviral vaccine design. PLoS Negl Trop Dis 8:e2719. https://doi.org/10.1371/journal.pntd.0002719.
47. Rostand KS, Esko JD. 1997. Microbial adherence to and invasion through proteoglycans. Infect Immun 65:1–8.
48. Hacker U, Nybakken K, Perrimon N. 2005. Heparan sulphate proteoglycans: the sweet side of development. Nat Rev Mol Cell Biol 6:530–541. https://doi.org/10.1038/nrm1681.
49. Tiwari V, Maus E, Sigar IM, Ramsey KH, Shukla D. 2012. Role of heparan sulfate in sexually transmitted infections. Glycobiology 22:1402–1412. https://doi.org/10.1093/glycob/cws106.
50. Schafer G, Blumenthal MJ, Katz AA. 2015. Interaction of human tumor viruses with host cell surface receptors and cell entry. Viruses 7:2592–2617. https://doi.org/10.3390/v7052592.
51. Gardner CL, Ebel GD, Ryman KD, Klimstra WB. 2011. Heparan sulfate binding by natural eastern equine encephalitis viruses promotes neurovirulence. Proc Natl Acad Sci U S A 108:16026–16031. https://doi.org/10.1073/pnas.1110617108.
52. Klimstra WB, Ryman KD, Johnston RE. 1998. Adaptation of Sindbis virus to BHK cells selects for use of heparan sulfate as an attachment receptor. J Virol 72:7357–7366.
53. Smit JM, Waarts BL, Kimata K, Klimstra WB, Bittman R, Wilschut J. 2002. Adaptation of alphaviruses to heparan sulfate: interaction of Sindbis and Semliki Forest viruses with liposomes containing lipid-conjugated heparin. J Virol 76:10128–10137. https://doi.org/10.1128/JVI.76.20.10128-10137.2002.
54. Bernard KA, Klimstra WB, Johnston RE. 2000. Mutations in the E2 glycoprotein of Venezuelan equine encephalitis virus confer heparan sulfate interaction, low morbidity, and rapid clearance from blood of mice. Virology 276:93–103. https://doi.org/10.1006/viro.2000.0546.
55. O'Donnell CD, Kovacs M, Akhtar J, Valyi-Nagy T, Shukla D. 2010. Expanding the role of 3-O-sulfated heparan sulfate in herpes simplex virus type-1 entry. Virology 397:389–398. https://doi.org/10.1016/j.virol.2009.11.011.
56. Shukla D, Liu J, Blaiklock P, Shworak NW, Bai X, Esko JD, Cohen GH, Eisenberg RJ, Rosenberg RD, Spear PG. 1999. A novel role for 3-O-sulfated heparan sulfate in herpes simplex virus 1 entry. Cell 99:13–22. https://doi.org/10.1016/S0092-8674(00)80058-6.
57. Shukla D, Spear PG. 2001. Herpesviruses and heparan sulfate: an intimate relationship in aid of viral entry. J Clin Invest 108:503–510. https://doi.org/10.1172/JCI200113799.
58. Dong LQ, Wang XQ, Guo YN, Wu J, Li S, Yu P, Wang Z. 2013. HS N-sulfation and iduronic acids play an important role in the infection of respiratory syncytial virus in vitro. Eur Rev Med Pharmacol Sci 17:1864–1868.
59. Zautner AE, Jahn B, Hammerschmidt E, Wutzler P, Schmidtke M. 2006. N- and 6-O-sulfated heparan sulfates mediate internalization of coxsackievirus B3 variant PD into CHO-K1 cells. J Virol 80:6629–6636. https://doi.org/10.1128/JVI.01988-05.
60. Xu Y, Martinez P, Seron K, Luo G, Allain F, Dubuisson J, Belouzard S. 2015. Characterization of hepatitis C virus interaction with heparan sulfate proteoglycans. J Virol 89:3846–3858. https://doi.org/10.1128/JVI.03647-14.
61. Kobayashi F, Yamada S, Taguwa S, Kataoka C, Naito S, Hama Y, Tani H, Matsuura Y, Sugahara K. 2012. Specific interaction of the envelope glycoproteins E1 and E2 with liver heparan sulfate involved in the tissue tropismatic infection by hepatitis C virus. Glycoconj J 29:211–220. https://doi.org/10.1007/s10719-012-9388-z.
62. Mohan A, Kiran DH, Manohar IC, Kumar DP. 2010. Epidemiology, clinical manifestations, and diagnosis of Chikungunya fever: lessons learned from the re-emerging epidemic. Indian J Dermatol 55:54–63. https://doi.org/10.4103/0019-5154.60355.
63. Kalia M, Chandra V, Rahman SA, Sehgal D, Jameel S. 2009. Heparan sulfate proteoglycans are required for cellular binding of the hepatitis E virus ORF2 capsid protein and for viral infection. J Virol 83:12714–12724. https://doi.org/10.1128/JVI.00717-09.
64. Holmborn K, Ledin J, Smeds E, Eriksson I, Kusche-Gullberg M, Kjellen L. 2004. Heparan sulfate synthesized by mouse embryonic stem cells deficient in NDST1 and NDST2 is 6-O-sulfated but contains no N-sulfate groups. J Biol Chem 279:42355–42358. https://doi.org/10.1074/jbc.C400373200.
65. Ringvall M, Kjellen L. 2010. Mice deficient in heparan sulfate *N*-deacetylase/*N*-sulfotransferase 1. Prog Mol Biol Transl Sci 93:35–58. https://doi.org/10.1016/S1877-1173(10)93003-2.
66. De La Guardia C, Lleonart R. 2014. Progress in the identification of dengue virus entry/fusion inhibitors. Biomed Res Int 2014:825039. https://doi.org/10.1155/2014/825039.
67. Douam F, Lavillette D, Cosset FL. 2015. The mechanism of HCV entry into host cells. Prog Mol Biol Transl Sci 129:63–107. https://doi.org/10.1016/bs.pmbts.2014.10.003.
68. Banfield BW, Leduc Y, Esford L, Visalli RJ, Brandt CR, Tufaro F. 1995. Evidence for an interaction of herpes simplex virus with chondroitin sulfate proteoglycans during infection. Virology 208:531–539. https://doi.org/10.1006/viro.1995.1184.
69. Hsiao JC, Chung CS, Chang W. 1999. Vaccinia virus envelope D8L protein binds to cell surface chondroitin sulfate and mediates the adsorption of intracellular mature virions to cells. J Virol 73:8750–8761.
70. Jinno-Oue A, Tanaka A, Shimizu N, Mori T, Sugiura N, Kimata K, Isomura H, Hoshino H. 2013. Inhibitory effect of chondroitin sulfate type E on the binding step of human T-cell leukemia virus type 1. AIDS Res Hum Retroviruses 29:621–629. https://doi.org/10.1089/aid.2012.0156.
71. Kato D, Era S, Watanabe I, Arihara M, Sugiura N, Kimata K, Suzuki Y, Morita K, Hidari KI, Suzuki T. 2010. Antiviral activity of chondroitin sulphate E targeting dengue virus envelope protein. Antiviral Res 88:236–243. https://doi.org/10.1016/j.antiviral.2010.09.002.
72. Mardberg K, Trybala E, Tufaro F, Bergstrom T. 2002. Herpes simplex virus type 1 glycoprotein C is necessary for efficient infection of chondroitin sulfate-expressing *gro2C* cells. J Gen Virol 83:291–300. https://doi.org/10.1099/0022-1317-83-2-291.
73. Argyris EG, Acheampong E, Nunnari G, Mukhtar M, Williams KJ, Pomerantz RJ. 2003. Human immunodeficiency virus type 1 enters primary human brain microvascular endothelial cells by a mechanism involving cell surface proteoglycans independent of lipid rafts. J Virol 77:12140–12151. https://doi.org/10.1128/JVI.77.22.12140-12151.2003.
74. Zhang X, Zheng Z, Shu B, Liu X, Zhang Z, Liu Y, Bai B, Hu Q, Mao P, Wang H. 2013. Human astrocytic cells support persistent coxsackievirus B3 infection. J Virol 87:12407–12421. https://doi.org/10.1128/JVI.02090-13.
75. Kim E, Okumura M, Sawa H, Miyazaki T, Fujikura D, Yamada S, Sugahara K, Sasaki M, Kimura T. 2011. Paradoxical effects of chondroitin sulfate-E on Japanese encephalitis viral infection. Biochem Biophys Res Commun 409:717–722. https://doi.org/10.1016/j.bbrc.2011.05.072.
76. Riblett AM, Blomen VA, Jae LT, Altamura LA, Doms RW, Brummelkamp TR, Wojcechowskyj JA. 2016. A haploid genetic screen identifies heparan sulfate proteoglycans supporting Rift Valley fever virus infection. J Virol 90:1414–1423. https://doi.org/10.1128/JVI.02055-15.
77. Schowalter RM, Pastrana DV, Buck CB. 2011. Glycosaminoglycans and sialylated glycans sequentially facilitate Merkel cell polyomavirus infectious entry. PLoS Pathog 7:e1002161. https://doi.org/10.1371/journal.ppat.1002161.
78. Gao C, Yu CK, Qu S, San MW, Li KY, Lo SW, Jiang L. 2012. The Golgi-localized Arabidopsis endomembrane protein12 contains both endoplasmic reticulum export and Golgi retention signals at its C terminus. Plant Cell 24:2086–2104. https://doi.org/10.1105/tpc.112.096057.
79. Hegelund JN, Jahn TP, Baekgaard L, Palmgren MG, Schjoerring JK. 2010. Transmembrane nine proteins in yeast and *Arabidopsis* affect cellular metal contents without changing vacuolar morphology. Physiol Plant 140:355–367. https://doi.org/10.1111/j.1399-3054.2010.01404.x.
80. Maeda Y, Ide T, Koike M, Uchiyama Y, Kinoshita T. 2008. GPHR is a novel anion channel critical for acidification and functions of the Golgi apparatus. Nat Cell Biol 10:1135–1145. https://doi.org/10.1038/ncb1773.
81. Carette JE, Guimaraes CP, Varadarajan M, Park AS, Wuethrich I, Godarova A, Kotecki M, Cochran BH, Spooner E, Ploegh HL, Brummelkamp TR. 2009. Haploid genetic screens in human cells identify host factors used by pathogens. Science 326:1231–1235. https://doi.org/10.1126/science.1178955.
82. Robinson MC. 1955. An epidemic of virus disease in Southern Province, Tanganyika Territory, in 1952-53. I. Clinical features. Trans R Soc Trop Med Hyg 49:28–32. https://doi.org/10.1016/0035-9203(55)90080-8.
83. Kishishita N, Takeda N, Anuegoonpipat A, Anantapreecha S. 2013. Development of a pseudotyped-lentiviral-vector-based neutralization assay for chikungunya virus infection. J Clin Microbiol 51:1389–1395. https://doi.org/10.1128/JCM.03109-12.
84. McKnight KL, Simpson DA, Lin SC, Knott TA, Polo JM, Pence DF, Johannsen DB, Heidner HW, Davis NL, Johnston RE. 1996. Deduced consensus sequence of Sindbis virus strain AR339: mutations contained in laboratory strains which affect cell culture and in vivo phenotypes. J Virol 70:1981–1989.
85. Okuno T, Okada T, Kondo A, Suzuki M, Kobayashi M, Oya A. 1968. Immunotyping of different strains of Japanese encephalitis virus by antibody-absorption, hemagglutination-inhibition and complement-fixation tests. Bull World Health Organ 38:547–563.

86. Collier WA, De Roever-Bonnet H, Hoekstra J. 1959. Changed virulence of the yellow fever virus vaccine strain 17D by a single mouse passage. Trop Geogr Med 11:75–79.
87. Horie K, Kokubu C, Yoshida J, Akagi K, Isotani A, Oshitani A, Yusa K, Ikeda R, Huang Y, Bradley A, Takeda J. 2011. A homozygous mutant embryonic stem cell bank applicable for phenotype-driven genetic screening. Nat Methods 8:1071–1077. https://doi.org/10.1038/nmeth.1739.
88. Kitamura T, Koshino Y, Shibata F, Oki T, Nakajima H, Nosaka T, Kumagai H. 2003. Retrovirus-mediated gene transfer and expression cloning: powerful tools in functional genomics. Exp Hematol 31:1007–1014. https://doi.org/10.1016/S0301-472X(03)00260-1.
89. Tani H, Morikawa S, Matsuura Y. 2011. Development and applications of VSV vectors based on cell tropism. Front Microbiol 2:272.
90. Matsuura Y, Tani H, Suzuki K, Kimura-Someya T, Suzuki R, Aizaki H, Ishii K, Moriishi K, Robison CS, Whitt MA, Miyamura T. 2001. Characterization of pseudotype VSV possessing HCV envelope proteins. Virology 286: 263–275. https://doi.org/10.1006/viro.2001.0971.
91. Uren AG, Mikkers H, Kool J, van der Weyden L, Lund AH, Wilson CH, Rance R, Jonkers J, van Lohuizen M, Berns A, Adams DJ. 2009. A high-throughput splinkerette-PCR method for the isolation and sequencing of retroviral insertion sites. Nat Protoc 4:789–798. https://doi.org/10.1038/nprot.2009.64.
92. Rong Y, Nakamura S, Hirata T, Motooka D, Liu YS, He ZA, Gao XD, Maeda Y, Kinoshita T, Fujita M. 2015. Genome-wide screening of genes required for glycosylphosphatidylinositol biosynthesis. PLoS One 10:e0138553. https://doi.org/10.1371/journal.pone.0138553.